Environmental Research 196 (2021) 110927

Contents lists available at ScienceDirect

Environmental Research

journal homepage: www.elsevier.com/locate/envres

Examining the status of improved air quality in world cities due to COVID-19 led temporary reduction in anthropogenic emissions

Srikanta Sannigrahi [a,*], Prashant Kumar [b,c], Anna Molter [a,d], Qi Zhang [e,f], Bidroha Basu [a], Arunima Sarkar Basu [a], Francesco Pilla [a]

[a] School of Architecture, Planning and Environmental Policy, University College Dublin Richview, Clonskeagh, Dublin, D14 E099, Ireland
[b] Global Centre for Clean Air Research (GCARE), Department of Civil and Environmental Engineering, Faculty of Engineering and Physical Sciences, University of Surrey, Guildford, GU2 7XH, United Kingdom
[c] Department of Civil, Structural & Environmental Engineering, Trinity College Dublin, Dublin, Ireland
[d] Department of Geography, School of Environment, Education and Development, The University of Manchester, USA
[e] Department of Earth and Environment, Boston University, Boston, MA, 02215, USA
[f] Frederick S. Pardee Center for the Study of the Longer-Range Future, Frederick S. Pardee School of Global Studies, Boston University, Boston, MA, 02215, USA

ARTICLE INFO

Keywords:
Air pollution
Google Earth Engine
COVID-19
Lockdown
Human mobility
TROPOMI

ABSTRACT

Clean air is a fundamental necessity for human health and well-being. Anthropogenic emissions that are harmful to human health have been reduced substantially under COVID-19 lockdown. Satellite remote sensing for air pollution assessments can be highly effective in public health research because of the possibility of estimating air pollution levels over large scales. In this study, we utilized both satellite and surface measurements to estimate air pollution levels in 20 cities across the world. Google Earth Engine (GEE) and Sentinel-5 Precursor TROPOspheric Monitoring Instrument (TROPOMI) application were used for both spatial and time-series assessment of tropospheric Nitrogen Dioxide (NO_2) and Carbon Monoxide (CO) statuses during the study period (1 February to May 11, 2019 and the corresponding period in 2020). We also measured Population-Weighted Average Concentration (PWAC) of particulate matter ($PM_{2.5}$ and PM_{10}) and NO_2 using gridded population data and in-situ air pollution estimates. We estimated the economic benefit of reduced anthropogenic emissions using two valuation approaches: (1) the median externality value coefficient approach, applied for satellite data, and (2) the public health burden approach, applied for in-situ data. Satellite data have shown that ~28 tons (sum of 20 cities) of NO_2 and ~184 tons (sum of 20 cities) of CO have been reduced during the study period. $PM_{2.5}$, PM_{10}, and NO_2 are reduced by ~37 (μg/m^3), 62 (μg/m^3), and 145 (μg/m^3), respectively. A total of ~1310, ~401, and ~430 premature cause-specific deaths were estimated to be avoided with the reduction of NO_2, $PM_{2.5}$, and PM_{10}. The total economic benefits (Billion US$) (sum of 20 cities) of the avoided mortality are measured as ~10, ~3.1, and ~3.3 for NO_2, $PM_{2.5}$, and PM_{10}, respectively. In many cases, ground monitored data was found inadequate for detailed spatial assessment. This problem can be better addressed by incorporating satellite data into the evaluation if proper quality assurance is achieved, and the data processing burden can be alleviated or even removed. Both satellite and ground-based estimates suggest the positive effect of the limited human interference on the natural environments. Further research in this direction is needed to explore this synergistic association more explicitly.

1. Introduction

As per the Ecosystem Services (ESs) definition of Millennium Ecosystem Assessment (MA, 2005), clean air is one of the fundamental needs of human lives (Ash et al., 2010; Baró et al., 2014; Schirpke et al., 2014; Charles et al., 2020). Air pollution has been reduced substantially during the COVID-19 lockdown period. Venter et al. (2020) had examined both tropospheric and ground air pollution levels using satellite data and a network of >10,000 air quality stations across the world and found 29% reduction in NO_2 (with 95% confidence interval −44% to −13%), 11% reduction in Ozone (O_3), and 9% reduction in $PM_{2.5}$ during the first two weeks of lockdown (Venter et al., 2020). Kerimray et al.

* Corresponding author.
E-mail address: srikanta.sannigrahi@ucd.ie (S. Sannigrahi).

https://doi.org/10.1016/j.envres.2021.110927
Received 15 September 2020; Received in revised form 7 February 2021; Accepted 19 February 2021
Available online 4 March 2021

(2020) study at Almaty, Kazakhstan, found that the city-scale lockdown (effective on March 19, 2020) has resulted in 21% reduction in $PM_{2.5}$. The CO (49% reduction) and NO_2 (35% reduction) concentration has also been reduced substantially (Kerimray et al., 2020). In the same period, an increase (15%) in O_3 levels is also observed in Almaty, Kazakhstan (Kerimray et al., 2020). Mahato et al. (2020) had reported a sharp reduction in air pollution in Delhi, one of the most polluted cities in the world. The author found that the concentration of PM_{10} and $PM_{2.5}$ in Delhi was reduced to 60% and 39%, compared to the air pollution levels in 2019. The concentration of other pollutants, such as NO_2 (−53%) and CO (−30%), have also been reduced substantially during the lockdown period. In addition to this, Mahato et al. study had observed a 40%–50% improvement in air quality in Delhi within the first week of lockdown. Bao and Zhang (2020) study combined air pollution and Intracity Migration Index (IMI) data for 44 cities in northern China and found that restriction on human mobility is strongly associated with the reduction of air pollution in these cities. The author found that the air quality index (AQI) in these cities is decreased by ~8%, as the concentration of five key air pollutants, i.e., SO_2, $PM_{2.5}$, PM_{10}, NO_2, and CO have decreased by ~7%, ~6%, ~14%, ~25%, and ~5%, respectively. Sicard et al. (2020) had observed that due to COVID-19 lockdown, NO_2 mean concentrations were reduced substantially in all European cities, which was ~53% at urban stations. During the same period, the mean concentrations of O_3 was reported to be increased at the urban stations in Europe, i.e., 24% increases in Nice, 14% increases in Rome, 27% increases in Turin, 2.4% increases in Valencia and 36% in increases in Wuhan (China). Otmani et al. (2020) study at Morocco using three-dimensional air mass backward trajectories and the HYSPLIT model found that PM_{10}, SO_2, and NO_2 has been reduced up to 75%, 49%, and 96% during the lockdown period. In the southeast Asian (SEA) countries, Kanniah et al. (2020) study found that in Malaysia, PM_{10}, $PM_{2.5}$, NO_2, SO_2, and CO concentrations have been decreased by 26–31%, 23–32%, 63–64%, 9–20%, and 25–31% during the lockdown period. Kumar et al. (2020a) examined the impacts of COVID-19 mitigation measures on the reduction of $PM_{2.5}$ in five Indian cities (Chennai, Delhi, Hyderabad, Kolkata, and Mumbai), using in-situ measurements from 2015 to 2020, and termed it as an 'anthropogenic emission switch-off' experiment, allowing to understand the baseline concentrations across various cities. Kumar et al. study found that during the lockdown period (25 March to 11 May), the $PM_{2.5}$ concentration in the selected cities has been reduced by 19–43% (Chennai), 41–53% (Delhi), 26–54% (Hyderabad), 24–36% (Kolkata), and 10–39% (Mumbai), respectively. This study also found that cities with higher traffic volume exhibited a more significant reduction of $PM_{2.5}$.

The level of air pollution has a severe impact on human health and overall well-being. Air pollution is responsible for nearly 5 million deaths each year globally (IHME 2018). In 2017, air pollution had contributed to 9% of total deaths, ranges from 2% in the highly developed country to a maximum of 15% in low-developed countries, especially in South and East Asia (IHME, 2018). Based on Disability-Adjusted Life Years (DALYs) statistics, which demonstrate of losing one year of good health due to either premature mortality or disability caused by any factors, it has been estimated that air pollution is the 5th largest contributor to overall disease burden, only after high blood pressure, smoking, high blood sugar, and obesity, respectively (IHME, 2018). The adverse impact of air pollution on human health is not only limited to (low)developing countries. In the European regions, nearly 193,000 deaths in 2012 were attributed to airborne particulate matter (Ortiz et al., 2017). In addition, it has been found that air pollution in China is accountable for 4000 deaths each day, i.e., 1.6 million casualties in 2016 (Wang and Hao, 2012; Rohde and Muller, 2015). Chen et al. (2020) found that reduction in $PM_{2.5}$ during the lockdown period helped to avoid a total of 3214 $PM_{2.5}$ related deaths (95% CI 2340–4087). Chen et al. (2020) also estimated that COVID-19 lockdown and resulted cut down of air pollution brought multi-faceted health benefits to non-COVID mortalities. Several research studies (Crouse et al., 2015; Dutheil et al., 2020a; He et al., 2020) have echoed the surmountable effects of air pollutants on human lives and found that an increase in 10 $\mu g/m^3$ of NO_2 per day will be responsible for a 0.13% increases of all-cause mortality (He et al., 2020). The mortality rate would be around 2% when the 5-day average NO_2 level would reach 10 $\mu g/m^3$ (Monica et al., 2011).

It is now well-established by many data-driven experiments that the accelerated rate of air pollution can have a substantial impact on overall human well-being. Many previous studies have examined the synergistic association between limited human activity and improved air quality across the scale (Chen et al., 2020; Kumar et al., 2020; Mahato et al., 2020; Ogen, 2020). These studies collectively suggested that temporary or periodic cessation of human activity could be a temporary solution for battling air pollution. However, the substantial reduction in air pollution during the lockdown is obvious and does not convey any revelation. Therefore, the co-benefits of this reduced anthropogenic emission need to be evaluated with an evidence-based approach to allow for the results to be used as a reference for future decision making and policy development. In addition to this, most of the previous studies have relied on ground-based measurements, and hence, strongly depend on the availability of publicly available data, which often creates obstacles while upscaling the approaches for larger scales. Therefore, this research work has made an effort to assess the air pollution levels of many key air pollutants after combining both satellite and ground measurements. This work aims to estimate the spatiotemporal variations in air pollution levels during the lockdown period from 1 February to 11 May in 2020 using a reference of the same period in 2019. The avoided premature mortality due to the reduction of air pollution levels and the corresponding economic benefits were also assessed using multiple economic valuation approaches. Finally, each city's population-weighted average air pollution concentration was estimated for the considered study period.

2. Materials and methods

2.1. Data source and data preparation

A total of 20 cities have been selected for evaluating the effect of lockdown on air quality. These cities are Antwerp, Barcelona, Brussels, Chicago, Cologne, Denver, Frankfurt, London, Los Angeles, Madrid, Milan, New York, Paris, Philadelphia, Rotterdam, Sao Paulo, Tehran, Turin, and Utrecht. These cities have been considered based on two criteria: high air pollution and high COVID-19 casualties. Most of the cities listed here are from European and American countries. These countries reported more COVID-19 casualties compared with the Asian and Latin American countries (as of May 11, 2020) (Sannigrahi et al., 2020; WHO, 2020). Both satellite remote sensing and ground air pollution data were utilized for evaluating the positive effects of lockdown on the air quality levels of these cities. For comparison purposes, the satellite-based air pollution was measured from 1 February to 11 May for both 2019 (lockdown equivalent period) and 2020 (lockdown period). The concentration of two key air pollutants, nitrogen dioxide (NO_2) and carbon monoxide (CO) was computed for both 2019 and 2020 using Sentinel 5 P data. Human mobility data Our World in Data including driving and transit for the selected cities, were collected from Apple (https://covid19.apple.com/mobility/) (city-scale) and Google (https://www.google.com/covid19/mobility/) (country-scale) mobility reports. In addition, the gridded human settlement data and population density data (pixel format) were collected from the Socio-Economic Data Application Center, National Aeronautics and Space Application data center (SEDAC, NASA). For evaluating the total air pollution reduction of these 20 cities in a more accurate way, the Geographical Information System (GIS) enabled city boundary (shapefile format) was extracted from the OpenStreetMap (OSM) application. Two consecutive steps were followed to get the boundary of these cities. First, the OSM relation identifier number (OSM id) was generated for all the 20 cities using

Nominatim, a search engine for OpenStreetMap data. Then, the OSM relation id of each city was used as an input in the OSM polygon creation application interface, which generates the geometry (both actual and simplified) of the relation id in poly, GeoJSON, WKT, or image formats. The formatted image geometry of the cities was then imported in the ArcGIS Pro software, and the city boundary was extracted using an automatic digitization function.

2.2. Estimation of air pollution

2.2.1. Sentinel 5 P TROPOMI data and TROPOMI Explorer Application

The ESA (European Space Agency) Sentinel-5 Precursor (S 5 P) is an example of low earth Sun-synchronous Orbit (SSO) polar satellite that provides information of tropospheric air quality, climate dynamics, and ozone layer concentration for the time period 2015–2022 (Veefkind et al., 2012). The ESA S 5 P mission is one of the few missions that is intended to measure air and climatic variability from the space-borne application. The S 5 P mission is associated with the Global Monitoring of the Environment and Security (GMES) space programme. The TROPOspheric Monitoring Instrument (TROPOMI) payload of S 5 P mission was designed to measure the tropospheric concentration of few key air pollutants, i.e., Ozone (O_3), NO_2, SO_2, CO, CH_4, CH_2O, and aerosol properties in line with Ozone Monitoring Instrument (OMI) and SCanning Imaging Absorption spectroMeter for Atmospheric CartograpHY (SCIAMACHY) programme (Veefkind et al., 2012). TROPOMI measures the concentration of key tropospheric constituents at a 7×3.5 km^2 spatial unit. This default spatial scale was downscaled into 1 km $\times$ 1 km scale for city-scale analysis and subsequent interpretation. In this study, the spatial and temporal variability of two key air pollutants was extracted and mapped from the TROPOMI measurements using the Google Earth Engine cloud platform. For this purpose, an interactive application called TROPOMI Explorer Application (https://showcase.earthengine.app/view/tropomi-explorer), was utilized to facilitate quick and easy S5P data exploration and to examine the changes in air pollution in both cross-sectional and longitudinal scale. Spatial visualization and time series charts for the selected air pollutants were prepared with the help of the TROPOMI Explorer application. The other accessories of this application, such as NO_2 time series inspector, NO_2 temporal comparison, NO_2 time-series animation, were also utilized for different computational purposes.

An extensive body of research has examined the applicability of satellite remote sensing in air pollution assessment from regional to global scale (Meng et al., 2016; Fernández-Pacheco et al., 2018; Alvarez-Mendoza et al., 2019; Basu et al., 2019; Zhang et al., 2019). Many studies have focused on monitoring Aerosol Optical Depth (AOD) using Moderate Resolution Imaging Spectroradiometer (MODIS) data to predict ambient fine particulate matter concentration (Zhang et al., 2010; Mehta et al., 2016). Since MODIS data has a low spatial resolution that often limits its application at fine-scale air pollution assessment, several moderate to high-resolution satellite data products, such as Landsat and Sentinel emerged to be an efficient alternative to measure pollution levels at city scale (Meng et al., 2016; Basu et al., 2019). Several approaches, including land use regression (Kloog et al., 2012; Basu et al., 2019), machine learning approaches – random forest (Fernández-Pacheco et al., 2018), stepwise regression, partial least squares regression (Alvarez-Mendoza et al., 2019), artificial neuronal network (Zhang et al., 2019), have been established to retrieve AOD and particulate matter concentration from Landsat and Sentinel data.

2.2.2. In-situ air pollution data

Ground monitored air quality data was collected from different governmental sources and open data repositories, including U.S. Environmental Protection Agency (https://www.epa.gov) (for Chicago, Denver, Detroit, Los Angeles, New York, and Philadelphia), European Environmental Agency (https://www.eea.europa.eu/) (for Antwerp, Barcelona, Brussels, Frankfurt, London, Madrid, Milan, Paris, Rotterdam, Utrecht), and OpenAQ (https://openaq.org/) (for Detroit and Los Angeles). The in-situ data was collected for three key air pollutants, i.e., NO_2, $PM_{2.5}$, and PM_{10}, for a fixed time period (1 February to 11 May) of both 2019 and 2020. The average concentration of different air pollutants was calculated to perform comparative assessment and subsequent interpretation. Since the in-situ air pollution data was not adequate for thorough spatial assessment, the same had not been used for validating satellite pollution estimates. The time series (2000–2020) air quality index (AQI) of the US cities (time-series historical data is not available for other cities) was also generated using the multilayer time plot function of EPA. The overall AQI values were sub-divided into six groups, i.e., good, moderate, unhealthy for sensitive population groups, unhealthy, very unhealthy, and hazardous, respectively. In addition, the single year AQI data was also extracted for the selected cities from the EPA. The number of unhealthy days for each pollutant was measured using the EPA AQI plot function. The combination of two different pollutants, such as CO and NO_2, $PM_{10,}$ and $PM_{2.5}$, was used to assess the yearly AQI status of the cities. As several studies reported the increment of O_3 due to the reduction of GHG emissions, this study also evaluated the O_3 exceedances for the current year compared to the average O_3 concentration of the last 5 and 20 years. This particular task was implemented using the EPA Ozone exceedances plot function (EPA, 2020). Table S1 provides the criteria of categorization for each index.

2.3. Environmental significance of improving air quality status

The accelerating increases of air pollution in cities is a major concern across the world (Mayer, 1999; Kim Oanh et al., 2006; Chan and Yao, 2008; Guttikunda et al., 2014; Pilla and Broderick, 2015; Abhijith et al., 2017; Rai et al., 2017; Zhu et al., 2020; Kumar et al., 2021; Rodríguez-Urrego and Rodríguez-Urrego, 2020). Various policies have been implemented for managing the city-based air pollution that mainly originated from anthropogenic activities from specific sources and sectors (Baró et al., 2014; Kumar et al., 2015, 2016, 2019a; Feng and Liao, 2016; Zhang et al., 2016). These include the Directive 2010/75/EU on industrial emissions, initiated by European Commission to define “Euro standards” for measuring the road vehicle emissions and the Directive 94/63/EC for calculating volatile organic compounds emissions from petrol storage (Baro et al., 2014). The reduction of these gaseous pollutants by green canopy has significant economic importance (Kumar et al., 2019). Two main ecosystem services, such as air quality regulation and climate/gas regulation, are mainly associated with air quality ecosystem services (Zhang et al., 2018, 2020). Several studies have calculated the economic values of NO_2, SO_2, CO reductions using various valuation approaches such as carbon tax, the social cost of carbon, shadow price method, marginal cost method. (Guerriero et al., 2016; Castro et al., 2017; Jeanjean et al., 2017; Bherwani et al., 2020). Since this study has considered the air pollution reduction at the city scale, the public health burden (utilized for in-situ data-based economic valuation) and mean externality valuation (utilized for satellite data-based economic valuation) approaches were utilized for estimating economic damage due to air pollution and for calculating the economic values of improved air quality (Matthews and Lave, 2000; Baro et al., 2014). Unit social damage price due to air pollution was estimated for 2020 using the US consumer price index (CPI) inflation calculator (U.S. Bureau of Labor Statistics, 2020). Additionally, using the most updated price conversion factors, the mean externality values for the key pollutants were estimated as 5149 and 956 US$ ton^{-1} for NO_2 and CO, respectively.

The public health burden valuation approach has been utilized in many studies for health impact assessment (COMEAP, 2010; Hu et al., 2015; Sahu and Kota, 2017; Etchie et al., 2018; Kumar et al., 2020a; Sharma et al., 2020). The calculation of public health burden and the associated economic burden was conducted by following three subsequent steps: first, estimation of population-weighted average concentration; second, estimation of health burden or a number of premature

mortality attributable to air pollution; and third, the economic burden due to excess air pollution and economic benefits subject to the reduction of air pollution levels during the lockdown period. The population-weighted average concentration (PWAC) (Ivy et al., 2008; Etchie et al., 2018; Park et al., 2020) was measured as follows:

$$PWAC = \frac{\sum_{x}(Pop_x \times C_x)}{\sum_{x} Pop_x} \quad (1)$$

where $Pop_x$is the population count of a pixel, $C_x$is the average concentration of NO_2, $PM_{2.5}$, PM_{10} (101 days, 1 February to 11 May in 2019 and 2020), $\sum_{x} Pop_x$is the total population count of the city, $PWAC$(μg/m^3) is the population-weighted average concentration. The PWAC was estimated using the ArcPy Python module. Gridded population data from SEDAC, NASA was utilized for this task. Pollution and gridded population data for the same time period were used for estimations of PWAC.

Following, the health burden (HB), which refers to premature deaths attributable to short-term exposure to air pollutants, was estimated for the study period. The reduction in HB (ΔHB) was also measured by calculating the difference between the previous and later HB estimates.

$$HB_x = AF \times B_x \times \sum_{x} Pop_x \quad (2)$$

$$AF = \left(\frac{RR_x - 1}{RR_x}\right) \quad (3)$$

$$\Delta HB = HB_{2019} - HB_{2020} \quad (4)$$

$$RR_i = e\left[\beta_i\left(C_i - C_{i,0}\right)\right], C_i > 0 \quad (5)$$

$$ER = RR - 1 \quad (6)$$

where $HB_x$is the health burden of city x, $AF$is the attributable fraction associated with the relative risk of each pollutant, $RR_i$is the relative risk of pollutant i, $B_x$is the baseline cause-specific mortality rate per 100,000 population. For calculating B_x, the country-wise cardiovascular and chronic respiratory baseline mortality rate was collected from the Global Burden of Disease study of 2017 (IHME, 2018).$Pop_x$is the population of city x derived from the SEDAC, NASA gridded population count data. $\Delta HB$is the difference in health burden (or avoidance of premature death due to the reduction in air pollution) from 1 February to May 11, 2020 compared to the same period in 2019. $HB_{2019}$and $HB_{2020}$is the health burden estimates in 2019 and 2020 (estimated for 1 February to 11 May time period). $\beta_i$is the exposure-response relationship coefficient, indicates the excess risk of health burden (such as mortality) per unit increase of pollutants. $\beta$is calculated 0.038%, 0.032%, 0.081%, 0.13%, and 0.048% per 1 μg/m^3 increases of $PM_{2.5}$, PM_{10}, SO_2, NO_2, and O_3, respectively (Hu et al., 2015; Chen et al., 2020; Kumar et al., 2020a; Sharma et al., 2020). $\beta$is calculated 3.7% per 1 mg/m^3 increases of CO. $C_i$is the concentration of pollutant i, $C_{i,0}$is the threshold concentration, below which the pollutant exhibits no obvious adverse health effects (i.e., RR = 1).

The economic burden (EB) and economic benefits of the reduced air pollution concentration were estimated using the value of statistical life (VSL) approach (Hu et al., 2015; Etchie et al., 2018). The VSL represents an individual's willingness to pay for a marginal reduction in the risk of dying. The economic benefits due to avoided premature mortality were estimated as follows:

$$EB_x = HB_x \times VSL_x \quad (7)$$

where EB_x is the economic benefit attributed to the reduction of air pollution and resulted in estimates of avoidable mortality, HB_x is the health burden estimates of city x, $VSL_x$is the value of statistical life of the country x that corresponds to the city. Since this study considers cities that cover many diversified economic setup and development background, a uniform income elastic global VSL estimates measured by Viscusi et al. (2017) was considered for the economic valuation and subsequent analysis. As city-specific VSL data is not available for many cities, the VSL estimates for the corresponding countries were taken for the analysis. The 2017 VSL values were converted to 2020 unit price for adjusting price fluctuation. The income adjusted VSL (Million US$) was estimated as Belgium (8, was used for Antwerp and Brussels), Spain (5, was used for Barcelona, Madrid), the USA (10, was used for Chicago, Denver, Detroit, Los Angeles, New York, and Philadelphia), Germany (8, was used for Cologne, Frankfurt), the UK (8, was used for London), Italy (6, was used for Milan and Turin), France (7, was used for Paris), the Netherlands (9, was used for Rotterdam and Utrecht), Brazil (2, was used for Sao Paulo), and Iran (1, was used for Tehran), respectively (Viscusi et al, 2017).

2.4. Examining human mobility and its connections with air pollution status

Due to the emergence of the COVID-19 pandemic, countries across the world imposed mandatory lockdowns to restrict human-mobility. This triggers the reduction of motorized traffic, which is one of the key sources of urban air pollution (Chinazzi et al., 2020; De Brouwer et al., 2020). Human mobility could accelerate the transmission of contagious diseases, especially when a larger fraction of the population daily commutes used public transport to sustain their essential daily journey (Sasidharan et al., 2020). Troko et al. (2011) study noted a statistically significant association between human mobility that is mainly attributed to public transport and transmissions of acute respiratory infections (ARI). Troko et al. (2011) also found that the use of public transport within the five days of symptom onset (Influenza) in the UK has increased the risk of ARI infection by six-times. To evaluate the effects of reduced human mobility on air pollution, the study presented in this paper utilized the human mobility data provided by Apple and Google (Drake et al., 2020; Wang and Yamamoto, 2020; Wellenius et al., 2020; Yilmazkuday, 2020). Apple mobility data includes three mobility components, i.e., driving, walking, and transit (public transport), respectively. The reduction of human mobility during the lockdown period was calculated from the baseline (13 January). Both positive and negative changes in human mobility were recorded in percentage form to eliminate calculation bias. Among the three mobility components, driving and transit was considered for the evaluation. Google mobility data was also used in this study which has six components (retail and recreation, grocery and pharmacy, parks, transits, workplace, and residential). This data is available from February 15, 2020 to recent date. Since Google mobility data is not available for city scale, the smallest scale (county/state) was taken for the analysis for which the mobility counts are available. This data is also prepared in percentage format to handle the calculation bias.

3. Results

3.1. Spatiotemporal changes in air pollution in different cities

Spatial distribution of tropospheric NO_2 and CO column (derived from Sentinel TROPOMI data) is analyzed and presented in Fig. 1 and Fig. S1. During the observation period, a sharp reduction in NO_2 and CO (μmol/m^2) is observed in all 20 cities. This could be due to the lockdown and resultant reduction of transportation and industrial emission. The maximum reduction in NO_2 is found for the European cities, such as Paris, Milan, Madrid, Turin, London, Frankfurt, Cologne, and American cities, such as New York, Philadelphia, etc. (Fig. 1). Moreover, the highest and lowest NO_2 reduction is found in Tehran and Sao Paulo. The CO concentration has also been reduced significantly during the study period. The highest reduction is recorded in Detroit, followed by Barcelona, London, Los Angeles, etc. (Fig. S1). On the other hand, during

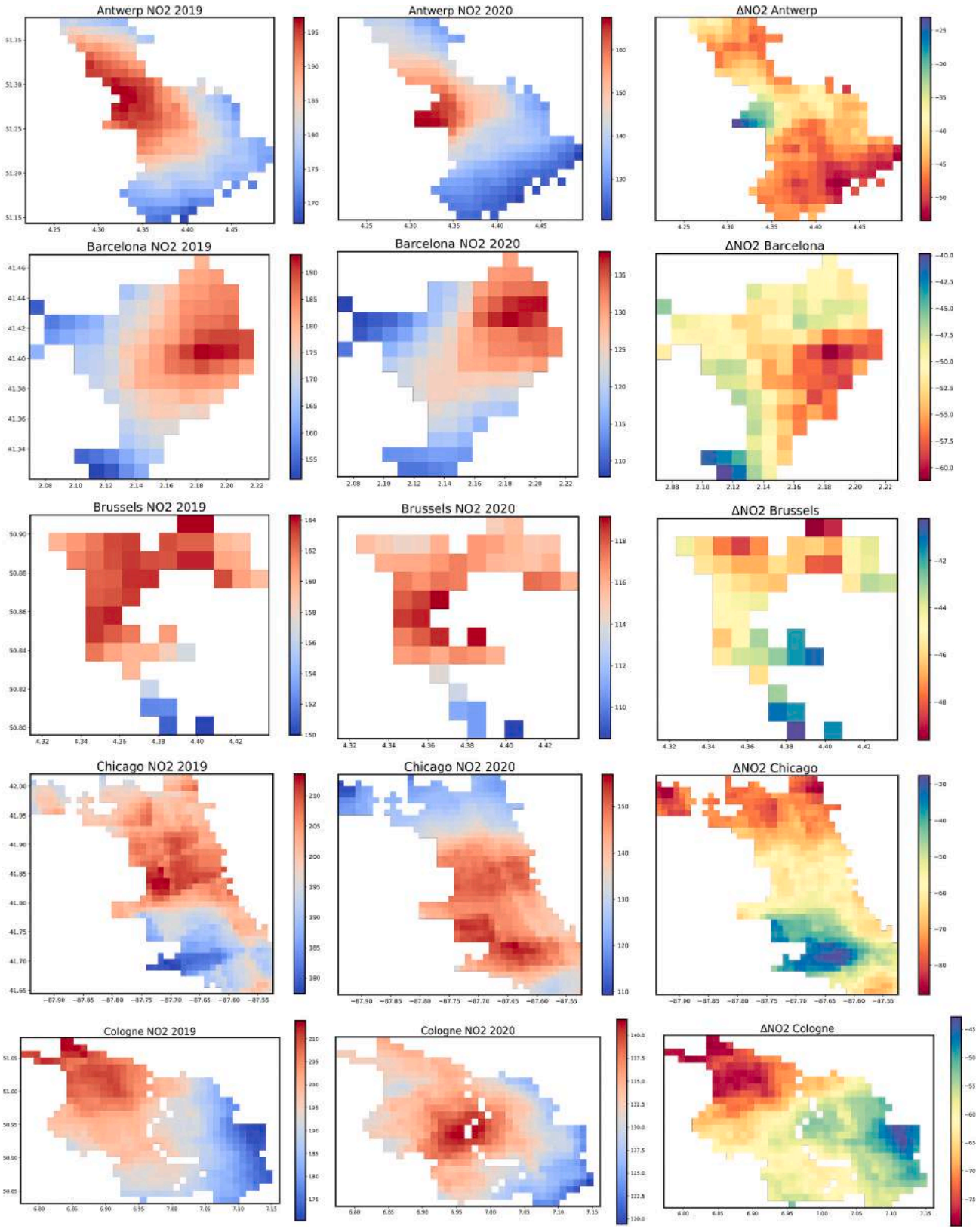

Fig. 1. Spatiotemporal variation (panel a and b) and changes in NO2 tropospheric column (μmol/m2) (panel c) in 20 cities during February 1 to May 11 derived from Sentinel 5 P TROPOMI sensor.

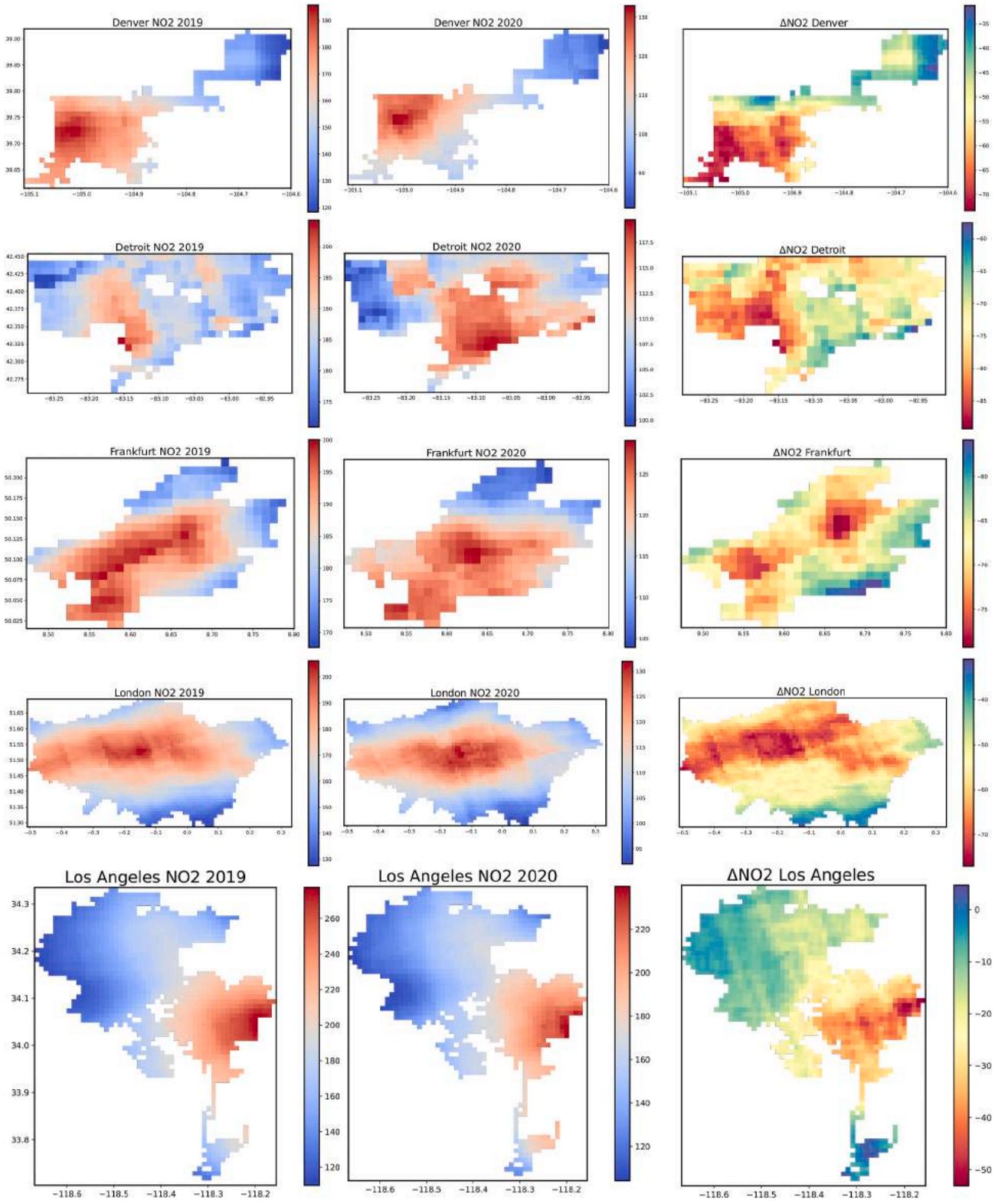

Fig. 1. (*continued*).

the same period, CO was increased in Cologne and Denver (Fig. S1).

Fig. 2 shows the average tropospheric NO_2 and CO column values from 1 February to 11 May. The average NO_2 (μmol/m^2) in 2019 and 2020 was found highest in Tehran, followed by Milan, New York, Paris, Turin, Chicago, Cologne, Philadelphia, etc. The lowest NO_2 column values (μmol/m^2) are found in Sao Paulo, Brussels, and Denver, respectively. The average CO values (μmol/m^2) was found highest in American cities, i.e., New York, Philadelphia, Detroit, Chicago, Los Angeles, while a comparably low tropospheric CO column (μmol/m^2) values are seen in Sao Paulo, Denver, Madrid, Barcelona, and Brussels (Fig. 2). Except for a few cities, NO_2 and CO column values have been reduced substantially during the study period (Fig. 3, Table 1). For NO_2, the highest reduction was detected in Paris (46%), followed by Detroit (40%), Milan (37%), Turin (37%), Frankfurt (36%), Philadelphia (34%),

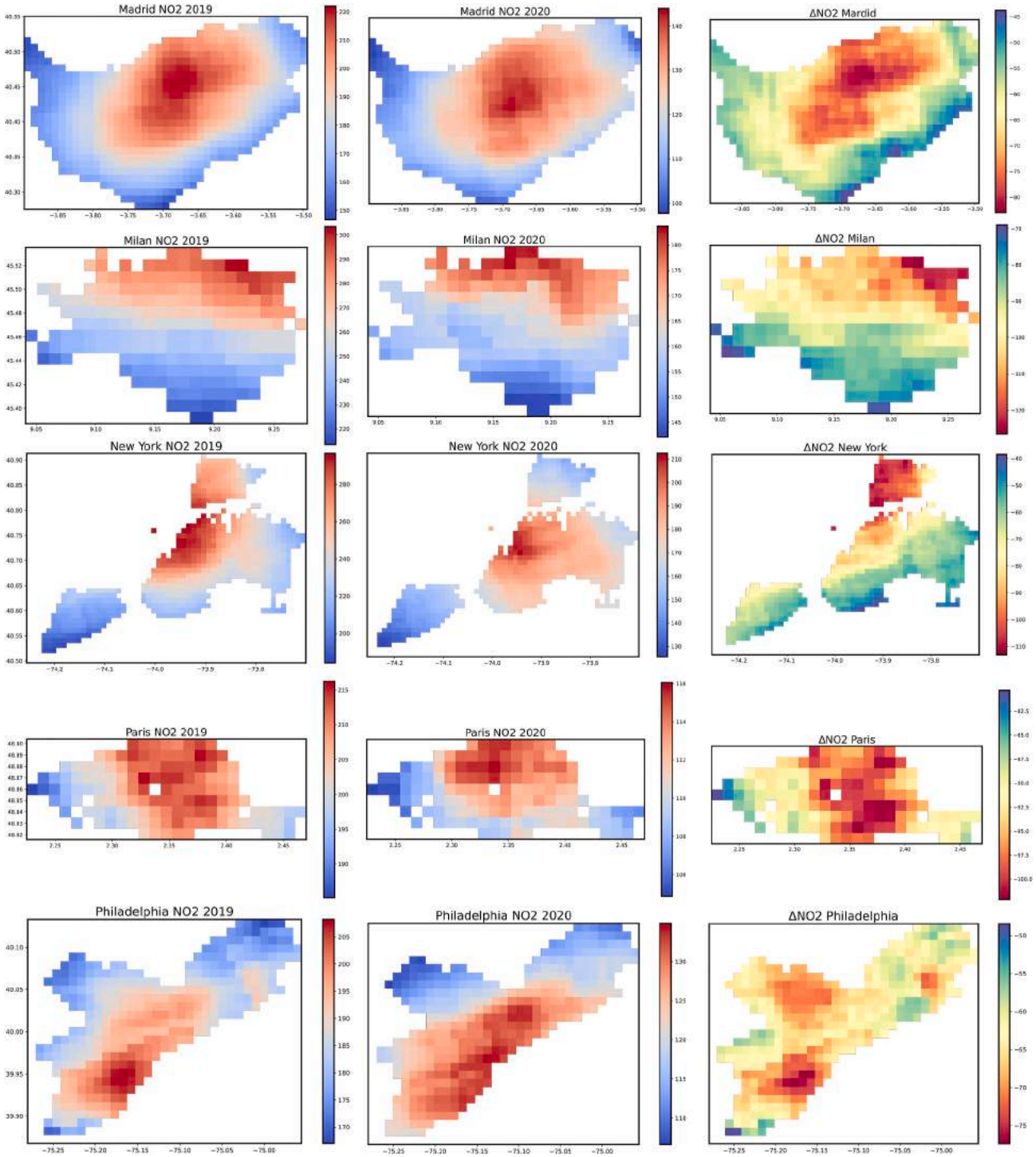

Fig. 1. (*continued*).

London (34%), and Madrid (34%), respectively. At the same time, a comparably lower reduction in NO_2 is observed in Los Angeles (11%), Sao Paulo (17%), Antwerp (24%), Tehran (25%), and Rotterdam (27%), respectively (Fig. 3). For CO, the maximum reduction was recorded for New York (4.24%), followed by Detroit (4.09%), Sao Paulo (3.88%), Philadelphia (3.45%), Milan (3.17%), Barcelona (2.86%), respectively. At the same time, a positive (increase) changes in CO were observed in Denver (1.92%), Cologne (0.49%), and Rotterdam (0.01%) (Fig. 3). The temporal variability of NO_2 is presented in Fig. 4, Fig. 5. Both median and interquartile range (IQR) values in Figs. 4 and 5 suggesting that NO_2 was decreased substantially.

Using the in-situ air pollution data, the concentration ($\mu g/m^3$) of NO_2, $PM_{2.5}$, and PM_{10} was evaluated and presented in Fig. 6 and Table 2. NO_2 concentration ($\mu g/m^3$) was found highest in American cities. On the contrary, the concentration of particulate matter ($PM_{2.5}$ and PM_{10}) was found highest in European cities. The changes (%) in NO_2, $PM_{2.5}$, and PM_{10} concentration from reference values (NO_2, $PM_{2.5}$, and PM_{10} concentration from 1 February to 11 May in 2019), was also measured (Fig. 7). The in-situ data suggest that the reduction in NO_2 was maximum in Brussels, followed by Paris and London. At the same time, $PM_{2.5}$ and PM_{10} were decreased substantially in London, Frankfurt, and Rotterdam. Additionally, $PM_{2.5}$ and PM_{10} concentration were found to

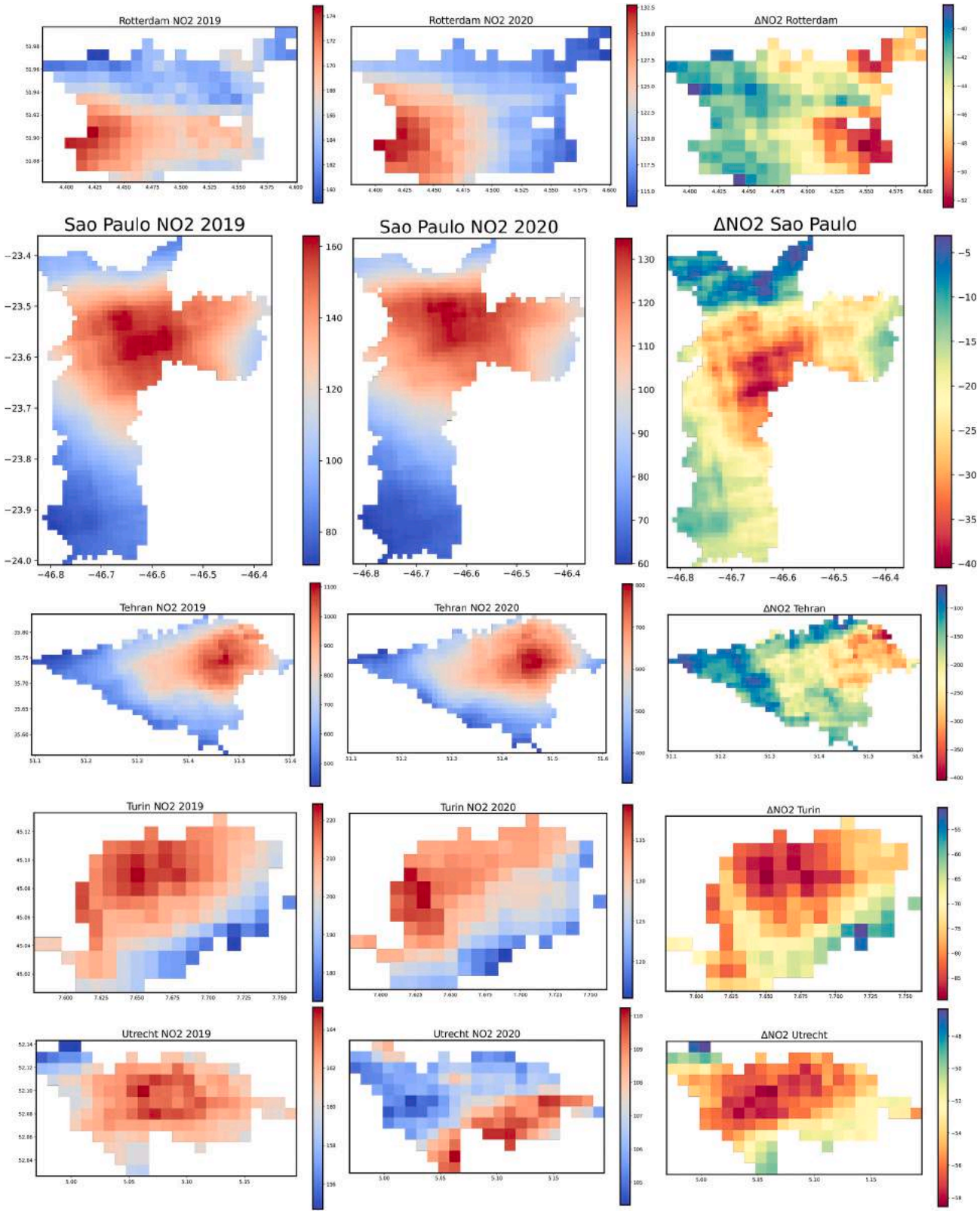

Fig. 1. (*continued*).

be increased in Los Angeles. The possible reason for this increment is discussed in the Discussion section.

3.2. Changes in human mobility

Using the Apple human mobility data, the driving, and transit driven mobility was calculated and presented in Fig. 8. Mobility on January 13 was taken as a baseline, and further changes in human mobility during

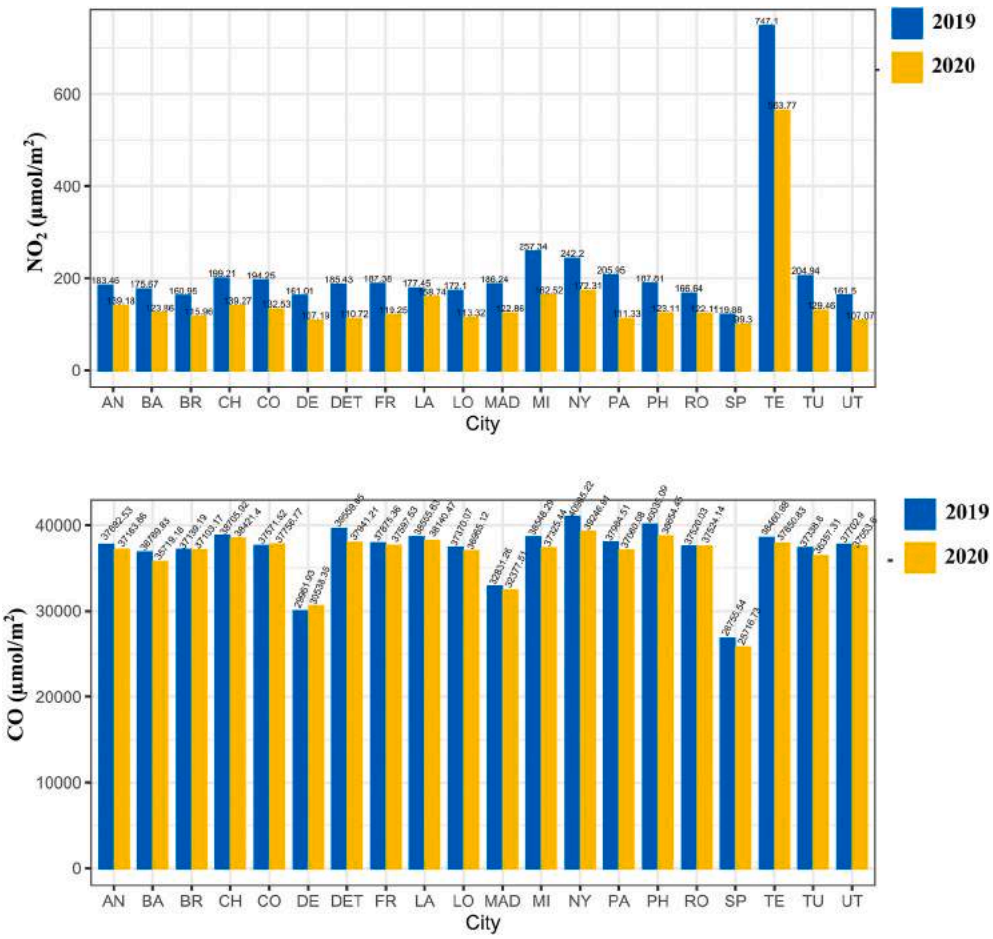

Fig. 2. NO2 and CO tropospheric column (µmol/m2) in 20 cities during February 1 to May 11 in 2019 and 2020, derived from Sentinel TROPOMI sensor.

the study period was calculated from the baseline mobility. The driving counts reduced most substantially in Paris, followed by Madrid, London, Antwerp, and Brussels (Fig. 8, Table S2). Whereas, such changes were comparably low in Chicago, Cologne, Denver, Los Angeles, New York (Fig. 8). Transit counts also reduced considerably in Paris, followed by Utrecht, Sao Paulo, New York, Milan, Chicago, Antwerp, and Brussels (Fig. 8). Google mobility records, which has six mobility components, i.e., retail and recreation, grocery and pharmacy stores, transit, parks and outdoor, workplace visitor, and time spent at home, were also utilized for country-wise assessment of human mobility changes (Fig. S2). Transport related mobilities were reduced most substantially in the Latin American countries, followed by a few Middle East and Southeast Asian countries, and American countries (Fig. S2; Fig. S3). Parks and outdoor activities were found to be reduced maximum in the Latin American countries and South Asian countries (Fig. S3). At the same time, outdoor activities are seen to be increased in a few European countries as well (Fig. S3). The highest reduction in retail and recreation was found in India, Turkey, the UK, and few Latin American countries due to lockdown and associated restrictive measures. (Fig. S4). Considering grocery and pharmacy-related mobilities, the highest reduction is being observed in the Latin American countries and a few European countries. Whereas grocery related mobility was found to be increased in the USA, few African and European countries (Fig. S4). Workplace related mobility is reduced considerably in Peru, Bolivia, India, Spain, Turkey, Saudi Arabia, USA, and Canada (Fig. S5). At the same time, such changes were positive in a few African countries (Mali, Niger, Mozambique, Zambia), Venezuela, and a few island countries (Fig. S5). Finally, using the Google real-time mobility information, another mobility component, i.e., time spent at home, was calculated (Fig. S5). As expected, due to lockdown and mandatory restrictive measures on human activities, people tend to spend more time at home, which also suggests that at most of the countries have taken timely decisions to control the pandemic. Except for a few European countries, peoples around the world limited their outdoor activities, which is supported by the results shown in Fig. S5.

3.3. Lockdown and improving status of air quality

Both public health burden (applied for in-situ data) and externality valuation (applied for Sentinel TROPOMI pollution data) approaches were utilized for assessing economic benefits and economic burden attributed to air pollution led cause-specific mortality (Table 3, Table 4, Table 5, Table S3; Table S4; Table S5). For satellite data-based economic assessment, the default unit (µmol/m^2) was converted to a mass unit (Ton) using the standard mass conversion approach (Borsdorff et al., 2018; Ialongo et al., 2020; Liu et al., 2020). Also, to estimate the total economic benefits of air pollution reduction, the difference in pollution concentration between the current year (1 February to 11 May in 2020) and the preceding year (1 February to 11 May in 2019) was computed. The per-unit economic benefits (US$) due to the reduction of air pollution was found maximum in Sao Paulo (49,709), followed by New York (49,447), Tehran (43,625), London (38,928), Detroit (22,585), Los Angeles (20240), Philadelphia (19188), Madrid (16,413), Chicago (13,222), Milan (10,034), Frankfurt (5854), Turin (5749), Antwerp (5039), Paris (4971), Barcelona (4116), Cologne (3915), Rotterdam (3401), Brussels (1876), and Utrecht (1675) (Table 4). The health burden and associated economic impacts of COVID-19 led reduction in NO_2, $PM_{2.5}$, PM_{10} concentrations across selected 20 cities were analyzed and

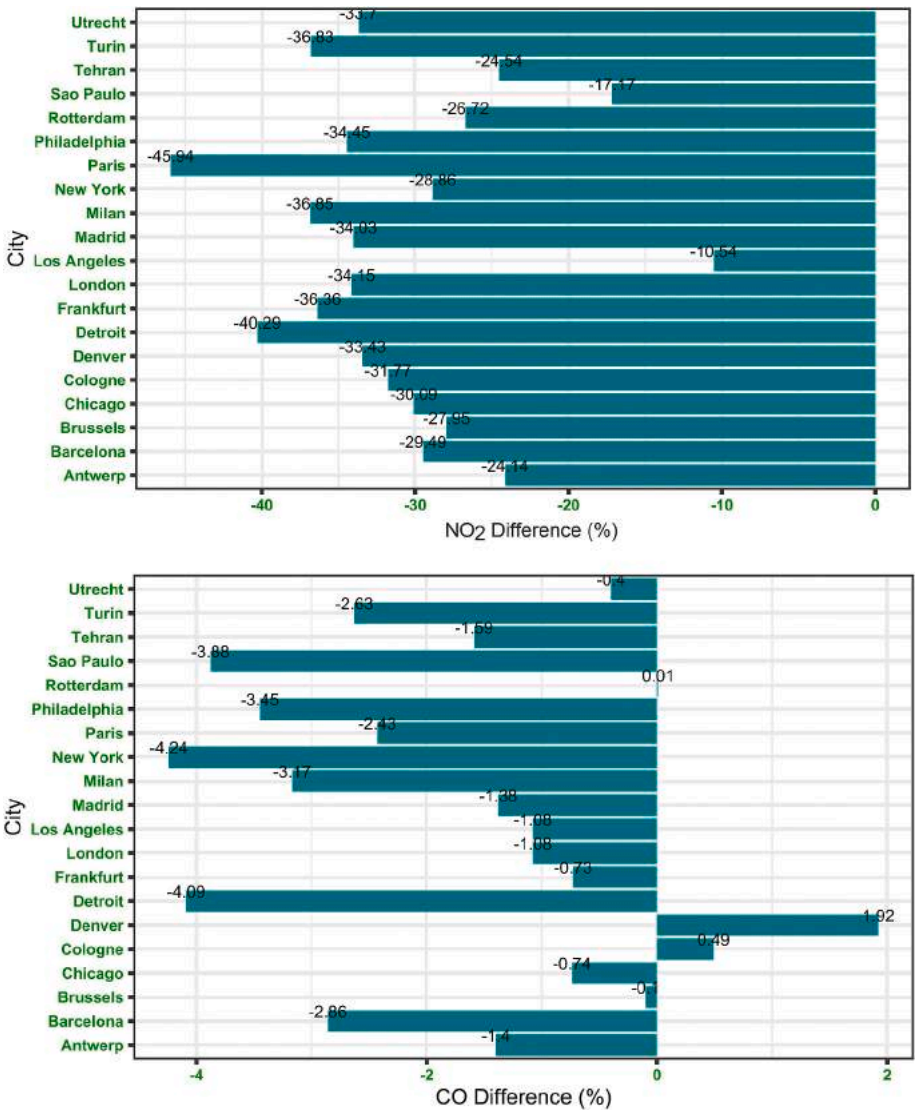

Fig. 3. Changes (%) in NO2 and CO during February 1 to May 11 in 2019 and 2020, derived from Sentinel 5 P TROPOMI data.

Table 1
Total emission (ton) of different air pollutants in 2019 and 2020 derived from Sentinel TROPOMI.

City	NO_2			CO		
	2019	2020	Difference (%)	2019	2020	Difference (%)
Antwerp	1.73	1.31	−24.14	215.83	212.80	−1.40
Barcelona	0.82	0.58	−29.49	104.91	101.91	−2.86
Brussels	1.20	0.86	−27.95	167.84	167.68	−0.10
Chicago	5.55	3.88	−30.09	656.87	652.04	−0.74
Cologne	3.62	2.47	−31.77	426.27	428.37	0.49
Denver	2.97	1.98	−33.43	336.58	343.06	1.92
Detroit	3.16	1.89	−40.29	409.95	393.18	−4.09
Frankfurt	2.14	1.36	−36.36	263.32	261.39	−0.73
London	12.45	8.20	−34.15	1644.88	1627.06	−1.08
Los Angeles	10.63	9.51	−10.54	1405.58	1390.45	−1.08
Madrid	5.18	3.42	−34.03	555.52	547.84	−1.38
Milan	2.15	1.36	−36.85	196.23	190.00	−3.17
New York	8.73	6.21	−28.86	899.48	861.33	−4.24
Paris	1.00	0.54	−45.94	112.10	109.37	−2.43
Philadelphia	3.17	2.08	−34.45	411.40	397.21	−3.45
Rotterdam	2.50	1.83	−26.72	342.27	342.31	0.01
Sao Paulo	8.39	6.95	−17.17	1139.46	1095.22	−3.88
Tehran	25.09	18.93	−24.54	786.14	773.67	−1.59
Turin	1.23	0.78	−36.83	136.12	132.54	−2.63
Utrecht	0.74	0.49	−33.70	104.73	104.32	−0.40

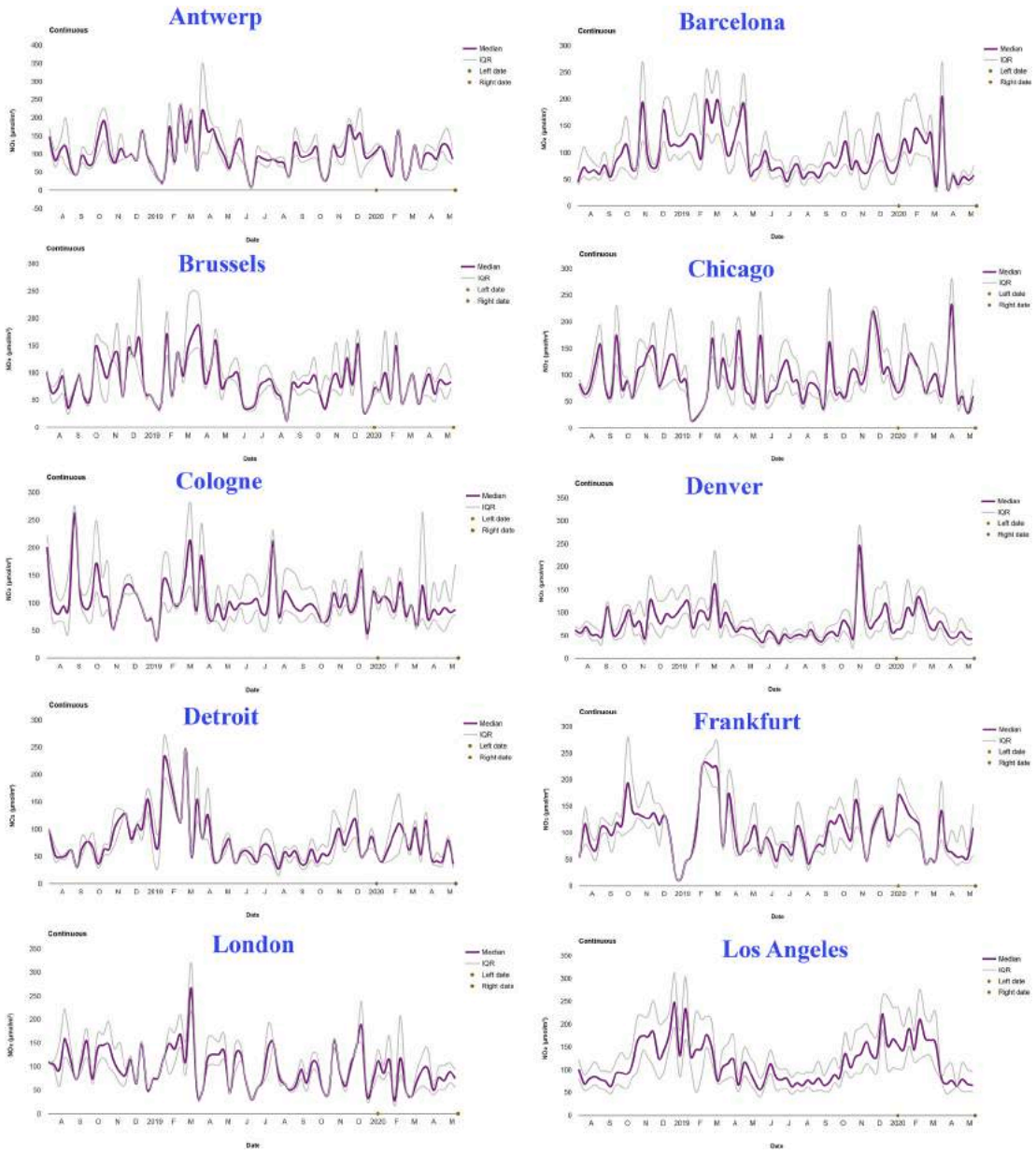

Fig. 4. Temporal variation in NO2 tropospheric column (μmol/m2) in the selected cities, derived from Sentinel 5 P TROPOMI data.

presented in Table 5. Health impacts are presented in terms of economic burden (indicates the increased levels of air pollution and resulted in cause-specific mortality) and economic benefits (related to reducing air pollution levels and avoided premature deaths). For NO_2, economic benefits (Million US$) were found highest in London, followed by New York, Paris, and Chicago. In comparison, monetary benefits were found minimum in Los Angeles and Utrecht. The economic benefits attributed to the reduction of $PM_{2.5}$ and PM_{10} were found highest in London, followed by New York, Paris, Chicago, Frankfurt, respectively. The city-wise population-weighted average concentration ($\mu g/m^3$), attributed to NO_2, $PM_{2.5}$, and PM_{10}, were estimated and presented in Fig. 9. The high PWAC value denotes the higher level of long term exposure to NO_2, $PM_{2.5}$, and PM_{10} and vice versa. Among the cities, the higher PWAC values (for NO_2) were estimated for the US cities (Denver, Detroit, New York, Los Angeles), compared to the European cities considered in this study. For both $PM_{2.5}$ and PM_{10}, the higher level of exposure was computed for the European cities (Milan, London, Paris, Antwerp, Barcelona). Due to the reduction of air pollution concentration, the average population exposed to $PM_{2.5}$, PM_{10}, and NO_2 was reduced substantially for all cities, except few US cities (Los Angeles and Philadelphia). The reduced level of exposure during the study period suggesting a strong synergistic association between controlled human interference and improved air quality across the world. The health burden (HB) estimates suggest that due to the reduction of air pollution, a total of ~1310 (NO_2), ~401 ($PM_{2.5}$), and ~430 (PM_{10}) premature cause-specific deaths have been averted. The economic benefits of this avoided mortality were measured as ~10, ~3.1, and ~3.3 Billion US$ for NO_2, $PM_{2.5}$, and PM_{10}.

4. Discussion

4.1. Relevance of satellite remote sensing in air pollution mapping

The ESA Sentinel 5 P TROPOMI real-time pollution data was successfully utilized for evaluating linkages between the temporary cessation of human interferences and improving air quality across the cities.

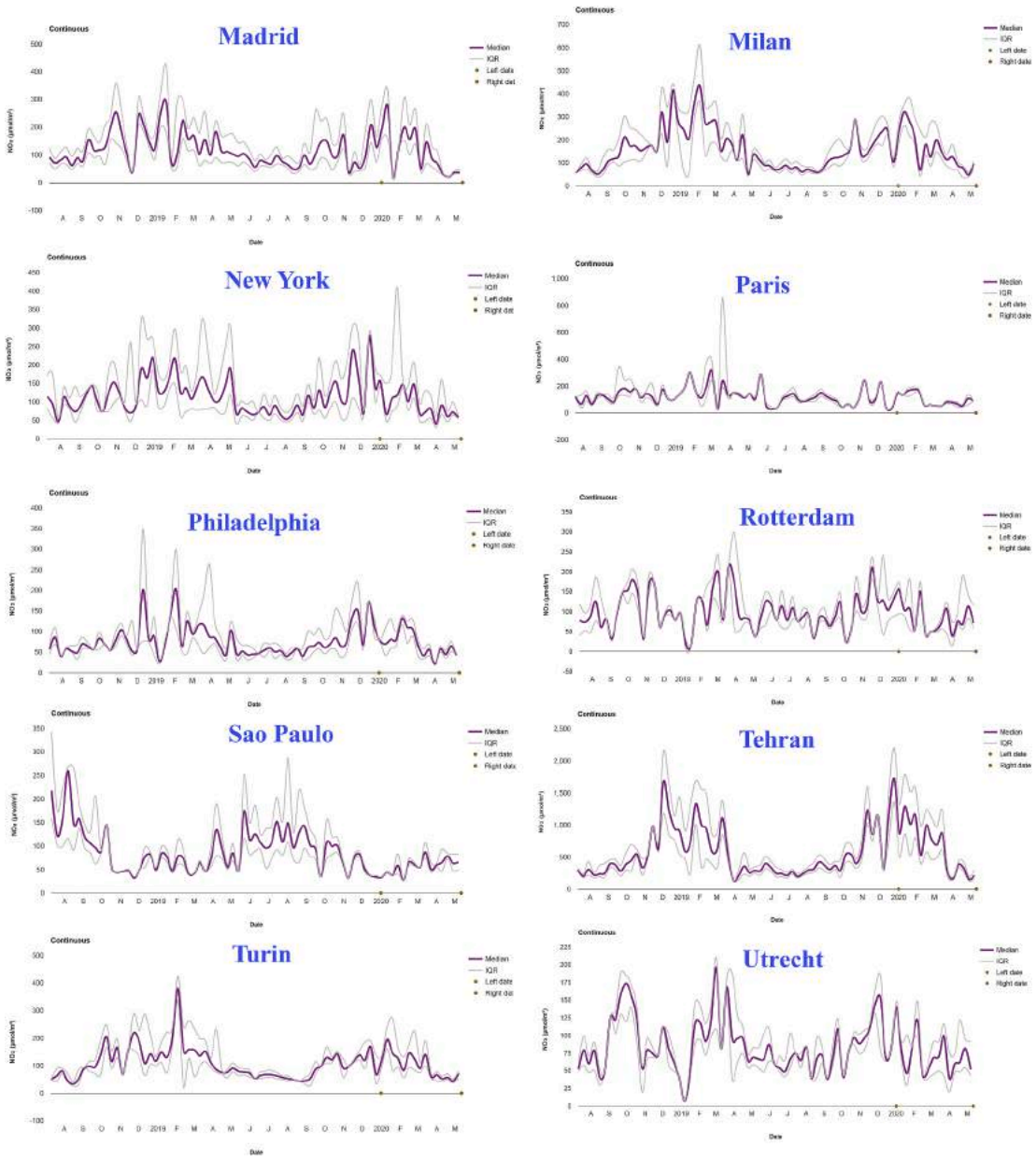

Fig. 4. (*continued*).

Sentinel 5 P satellite mission is one of the finest space-borne applications that provide the crucial key information of air quality, Ozone, ultra-violate radiation, and climate monitoring and forecasting (ESA, 2020). TROPOMI widens the application of the satellite air pollution observation and works in line with other global missions, i.e., SCIAMACHY (2002–2012), GOME-2 (since 2007), and OMI (since 2004) (Lorente et al., 2019). This data has been used for many purposes, including air pollution measurement (Borsdorff et al., 2018; Zheng et al., 2019; Shikwambana et al., 2020), epidemiological studies (Chen et al., 2020; Dutheil et al., 2020b; Gautam, 2020; Muhammad et al., 2020; Ogen, 2020; Shehzad et al., 2020); monitoring global volcano (Valade et al., 2019), demographic analysis (Kaplan and Yigit, 2020), evaluating sun-induced chlorophyll fluorescence (SIF) (Guanter et al., 2015), estimation of volcanic sulfur dioxide emission (Theys et al., 2019), etc. In addition, the advent of Google Earth Engine cloud-based functionality in handling the large volume of spatial data facilitates the application of satellite images for timely decision making and offering cost-benefit solutions to many environmental problems. Evaluating the reliability of remote sensing data is always a matter of concern. Many studies across the world have evaluated the reliability of Sentinel 5 P pollution data with ground measurements. Lorente et al. (2019) have examined the reliability of Sentinel TROPOMI tropospheric column NO_2 with in-situ (ground NO_2 boundary layer height over the Eiffel Tower was used in this purpose) data and found a very good agreement ($R^2 = 0.88$) between the two estimates. Griffin et al. (2019) study on validating TROPOMI data with aircraft and surface in situ NO_2 observations over the Canadian oil sands found that the TROPOMI vertical NO_2 column values are strongly correlated ($R^2 = 0.86$) with the aircraft and ground in situ NO_2 observations with a low bias (15–30%).

4.2. Reduced anthropogenic emission and improving air quality status across the cities

Air pollution levels in the urban region are mainly influenced by the local emission of pollutants. For example, Zeng et al. (2018) found that ~75% of the daytime O_3 concentration in Wuhan in summer 2016 was

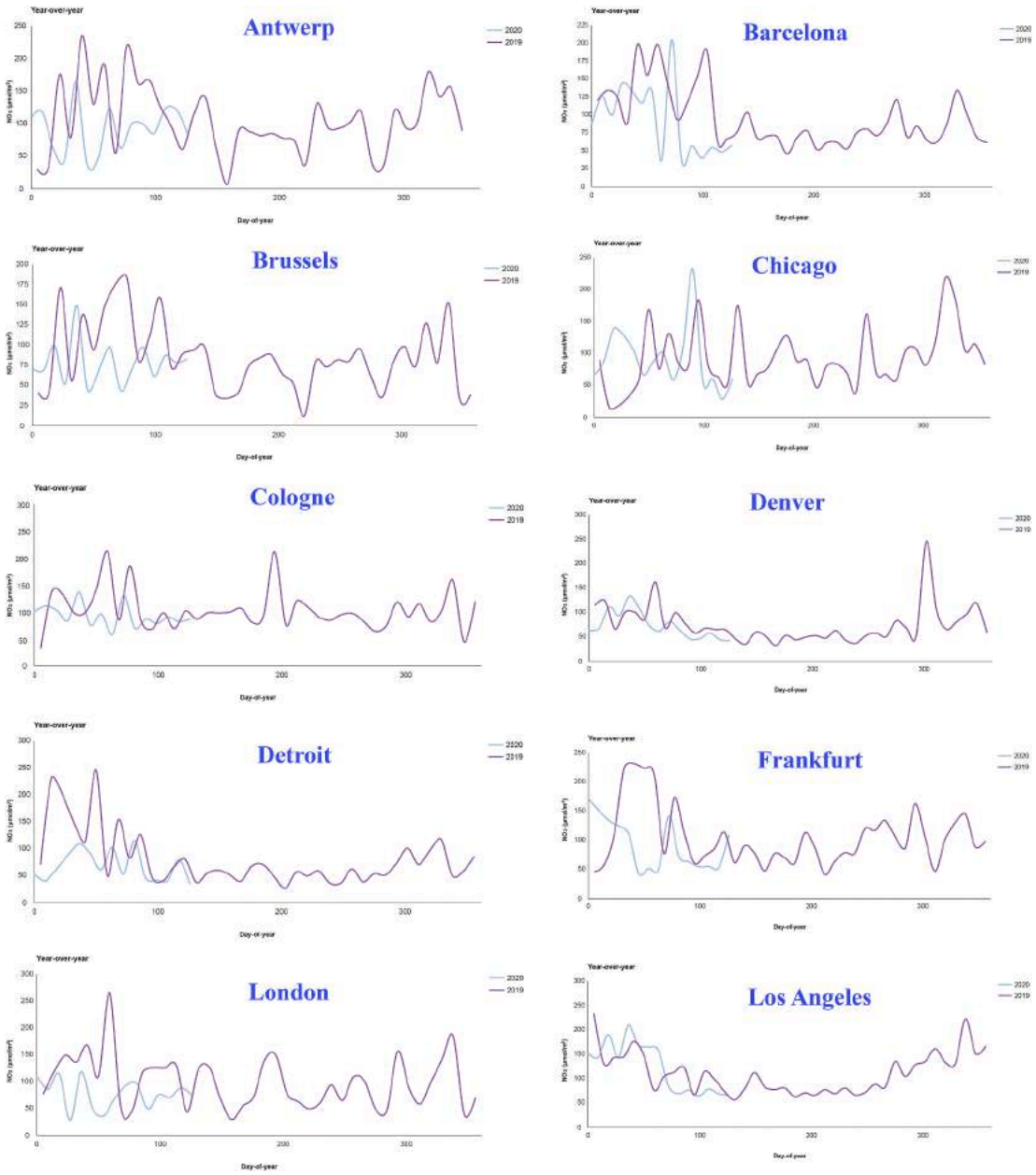

Fig. 5. Variation in NO2 tropospheric column (μmol/m2) in the selected cities during the study period in 2019 and 2020, derived from Sentinel 5 P TROPOMI data.

caused by localized photochemical formation. In cities, the main air pollutants of concern to public health are particulate matter ($PM_{2.5}$ and PM_{10}), NO_2, and tropospheric ozone (O_3). Both satellite and in-situ data suggest a considerable reduction in air pollution in all the 20 cities considered in this study. However, such reduction is not consistent among the cities: it was found to be very high over the European cities (for all three pollutants, i.e., $PM_{2.5}$ and PM_{10}, NO_2), and comparably low over the US cities. NO_2 concentration was reduced most significantly (>-40%) in Brussels and Paris, followed by −35% to −40% in Barcelona and London, −25% to −35% in Rotterdam, Antwerp, Madrid, Utrecht, −15%–25% in Milan, Frankfurt, Detroit, −5%–15% in New York, Denver, Chicago, and less than −5% in Los Angeles, respectively. During the same period, an incremental trend of NO_2 was observed in Philadelphia. Several studies also noted that NO_2 declined substantially during the COVID-19 time compared to historical years. Berman and Ebisu (2020) observed a statistically significant reduction in NO_2 (25.5% reduction with an absolute decrease of 4.8 ppb) in the continental USA from March 13 to April 21 in 2020 compared to average NO_2 concentration ($\mu g/m^3$) during 2017–2019. Baldasano (2020) estimated that reduction in NO_2 concentrations in Barcelona and Madrid (Spain) during the lockdown (March 2020) was 50% and 62%, which is in line with the findings of the present research. Using both satellite and in-situ data, Chen et al. (2020) observed that NO_2 concentration had been reduced substantially in China (12·9 $\mu g/m^3$). Venter et al. (2020) have analyzed ground-level measurements from >10,000 air quality stations in 34 countries and recorded a substantial NO_2 reduction (60%, 11 $\mu g/m^3$ in absolute terms) during the COVID lockdown dates.

In the urban region, NO_2 is mainly produced by human activities, including traffic emission, fuel combustion, and partly from industrial emission. EEA (2019) documented that in Europe, transport sector (road transport contributed to 39% of total emission, non-road transport contributed to 8% of total emission) is the most significant contributor to NOx emissions, followed by commercial, institutional and households emission, contributed to 14% of total NO_2 emission (EEA, 2019).

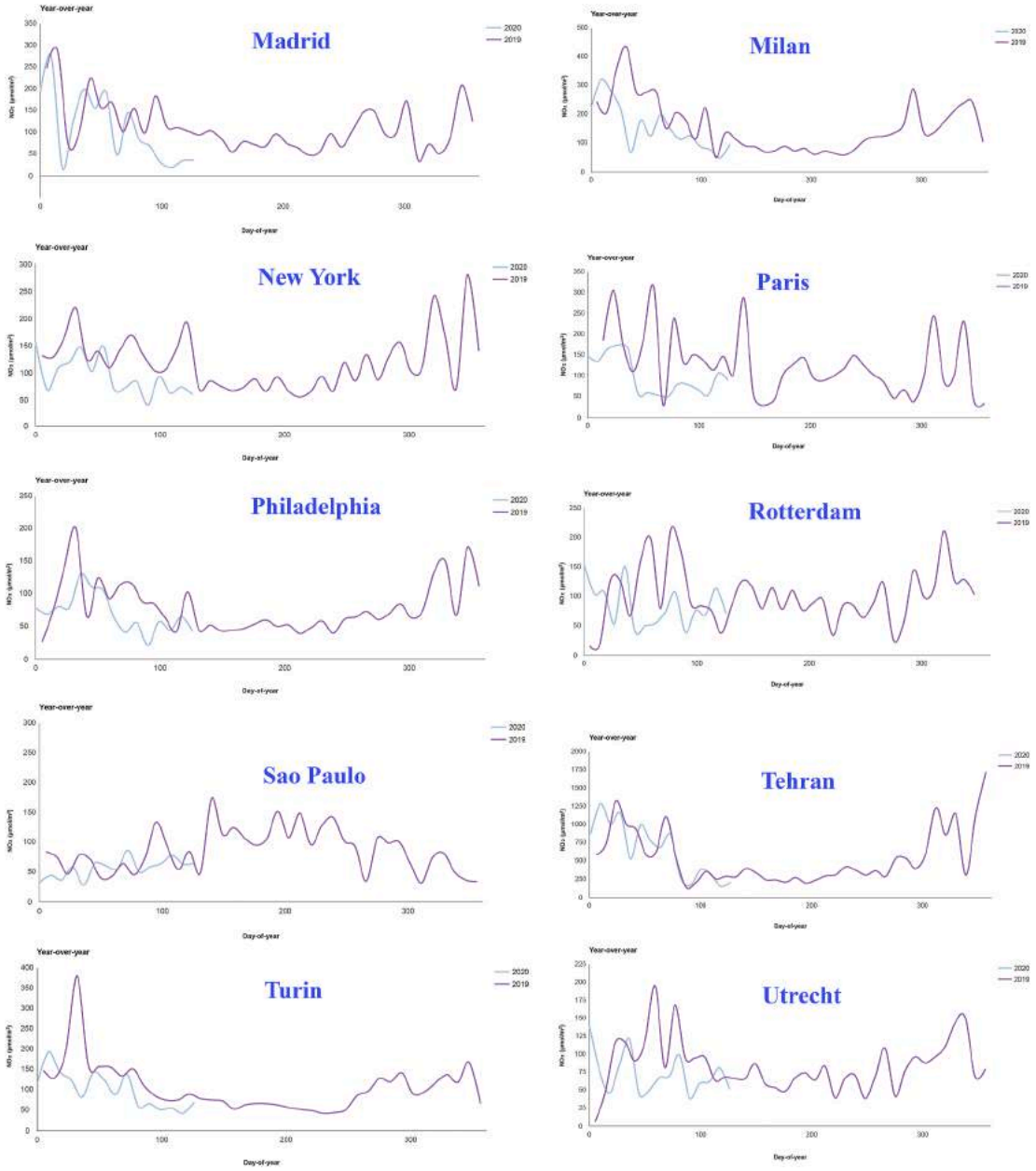

Fig. 5. (*continued*).

Additionally, in urban regions, the higher level of NO_2 concentration is mostly evident in cities with higher motorized traffic share, industrial regions, and densely populated areas (Zoran et al., 2020). Since we observed a drastic reduction in human mobility, including driving and transit during the observation period, the reduced level of traffic emission could therefore be linked to the decreasing trend of NO_2 observed in the European cities. The reduction of other sectorized emissions, such as industrial emission and commercial, institutional, and household emission, can also be associated with changes in NO_2 observed in these European cities. Kumar et al. (2020a) study on Indian cities noted that among all the influencing factors, including lockdown strictness, switch-off time to halt human activities, local meteorological condition, reduction in road traffic volume was found to be the most influential factor for explaining the variation in air pollution across cities.

Among the cities, the highest NO_2 reduction (−41%) was recorded in Brussels. Fierens et al. (2011) reported that air pollution in Brussels is strongly associated with traffic-related pollutants. Apple's mobility report also shows a substantial reduction in road traffic (−47% in driving and −25% in transit) in Brussels. Thus, the reduced level of road traffic volume could explain the noteworthy reduction of NO_2 concentration observed in Brussels. The second highest reduction in NO_2 concentration was recorded in Paris (−40.6%). In Paris, traffic and residential sectors are the main source of NO_2 pollution (Connerton et al., 2020). Traffic corresponds to 69% of NOx emissions, 36% of PM_{10} emissions, and 35% of $PM_{2.5}$ emission (Connerton et al., 2020). At the same time, the other contributing factors, such as the residential sector, contributes to 21% of total NOx emissions, 41% of total PM_{10} emissions, and 49% of total $PM_{2.5}$ emissions (Connerton et al., 2020). Other European capital cities, such as London, Barcelona, Madrid have also witnessed a drastic reduction in NO_2 concentration during the studied period. Reduction in road traffic and meteorological factors could be linked with this reduced NO_2 concentration observed in this study (Berman and Keita, 2020; Muhammad et al., 2020; Sharma et al., 2020). The NO_2 concentration in the US cities has not been changed significantly during the study period. Among the six US cities, the negative NO_2 changes were found lowest in Los Angeles (0.16%), followed by

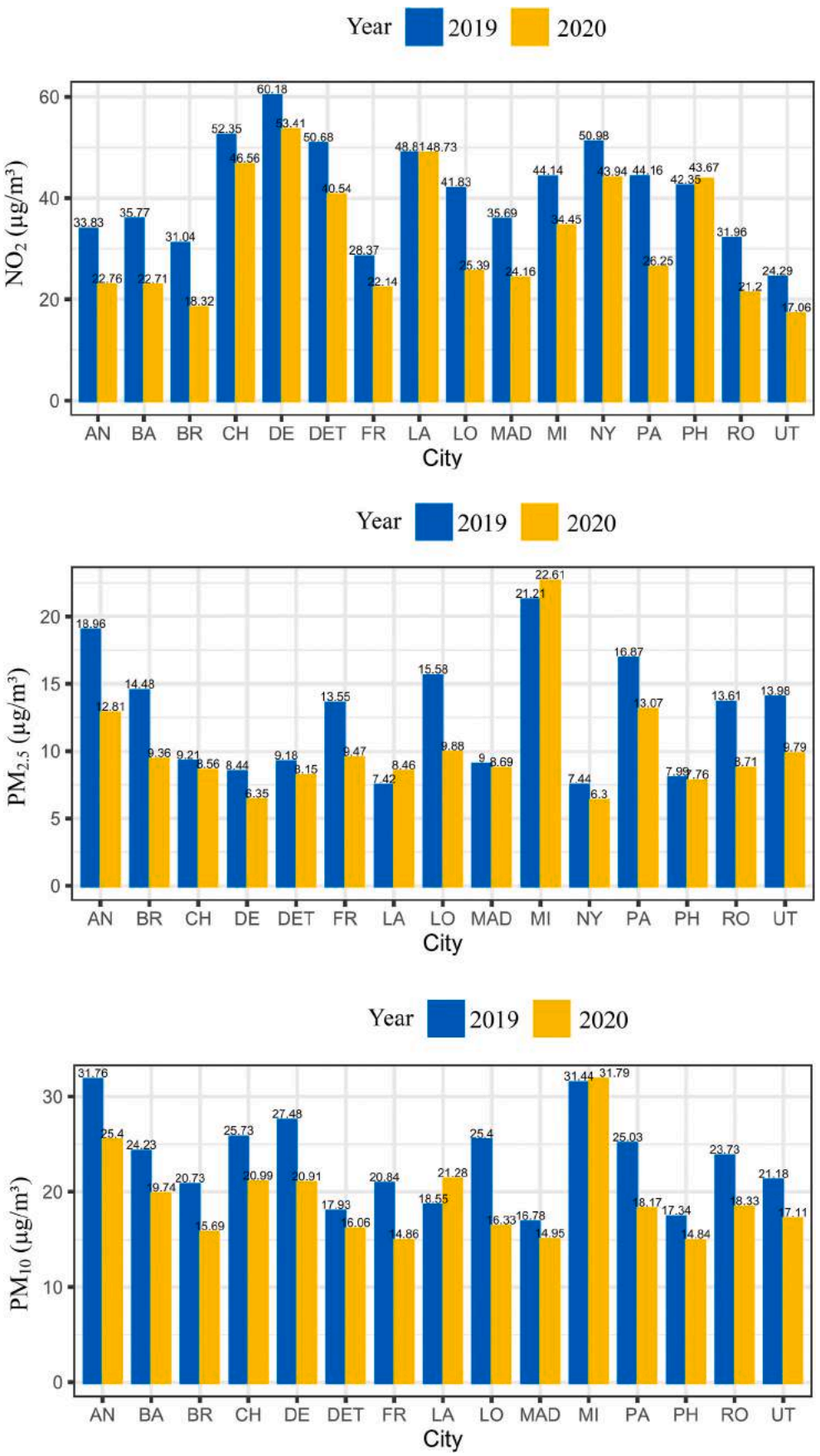

Fig. 6. NO2, PM2.5, and PM10 concentration (µg/m3) in selected cities during February 1 to May 11 in 2019 and 2020, derived fromin-situ data.

Table 2
NO2, PM2.5, and PM10 concentration (μg/m3) during the study period (1 February to 11 May) in 2019 and.

	NO_2 (μg/m^3)			PM_{10} (μg/m^3)			$PM_{2.5}$ (μg/m^3)		
	2019	2020	Δ NO_2 (%)	2019	2020	Δ PM_{10} (%)	2019	2020	Δ PM_{25} (%)
Antwerpen	33.83	22.76	−32.72	31.76	25.40	−20.02	18.96	12.81	−32.44
Barcelona	35.77	22.71	−36.50	24.23	19.74	−18.52	–	–	–
Brussels	31.04	18.32	−40.98	20.73	15.69	−24.28	14.48	9.36	−35.32
Chicago	52.35	46.56	−11.08	25.73	20.99	−18.42	9.21	8.56	−7.03
Denver	60.18	53.41	−11.26	27.48	20.91	−23.92	8.44	6.35	−24.81
Detroit	50.68	40.54	−20.01	17.93	16.06	−10.44	9.18	8.15	−11.22
Frankfurt	28.37	22.14	−21.95	20.84	14.86	−28.71	13.55	9.47	−30.10
London	41.83	25.39	−39.31	25.40	16.33	−35.73	15.58	9.88	−36.56
Los Angeles	48.81	48.73	−0.16	18.55	21.28	14.70	7.42	8.46	13.98
Madrid	35.69	24.16	−32.32	16.78	14.95	−10.88	9.00	8.69	−3.40
Milan	44.14	34.45	−21.96	31.44	31.79	1.13	21.21	22.61	6.57
New York	50.98	43.94	−13.80	–	–	–	7.44	6.30	−15.33
Paris	44.16	26.25	−40.55	25.03	18.17	−27.40	16.87	13.07	−22.55
Philadelphia	42.35	43.67	3.11	17.34	14.84	−14.40	7.99	7.76	−2.96
Rotterdam	31.96	21.20	−33.66	23.73	18.33	−22.78	13.61	8.71	−36.01
Utrecht	24.29	17.06	−29.77	21.18	17.11	−19.21	13.98	9.79	−29.95

Chicago (~11%), Denver (~11%), New York (~14%), and Detroit (~20%), respectively. During the same period, NO_2 concentration was found to be increased in Philadelphia (~3%). Meteorological factors could be responsible for these irregularities detected in these cities (Chauhan and Singh, 2020; Goldberg et al., 2020; Kumar et al., 2020a).

Similar to NO_2, a substantial reduction in particulate matter ($PM_{2.5}$ and PM_{10}) was observed for all the selected cities. The highest reduction (>35%) in $PM_{2.5}$ was recorded for London, Rotterdam, and Brussels, followed by 25%–35% reduction in Antwerp, Frankfurt, Utrecht, 15%–25% reduction in Denver, Paris, New York, 5%–15% reduction in Detroit, Chicago), and <5% reduction in Madrid and Philadelphia, respectively. On the other hand, $PM_{2.5}$ was recorded to be increased in Los Angeles and Milan. While, for PM_{10}, the maximum decline was observed over the European cities, with ranges >35% (London), 25%–35% (Paris, Frankfurt), 15%–25% (Brussels, Denver, Rotterdam, Antwerp, Utrecht, Barcelona, Chicago), 5%–15% (Detroit, Madrid, Philadelphia). In Milan and Los Angeles, PM_{10} concentration was found to be increased during the studied period. Urrego and Urrego (2020) study analyzed the $PM_{2.5}$ concentration in the 50 most polluted capital cities in the world. Urrego et al. stated that in Asian cities, the highest reduction in $PM_{2.5}$ was recorded in Delhi (40% reduction during the quarantine week), followed by Tehran (39%), Kabul, Colombo and Tashkent (28%), Dhaka (24%), and Astana (18%), respectively. Wang et al. (2020) examined the effect of lockdown in $PM_{2.5}$ concentration in Beijing, Shanghai, Guangzhou, and Wuhan and found a marked reduction in $PM_{2.5}$ emissions, which was mainly attributed to the partial/complete closure of transportation and industries across the cities. Guevara et al. (2020) study on time-resolved emission reductions in Europe during the COVID-19 lockdown period found that during the most severe lockdown period, average $PM_{2.5}$ emission was reduced −7% at the EU-30 level. Sicard et al. (2020) study on analyzing air pollution reduction on four European and one Asian city have found that at all stations, PM_{10} concentrations were decreased by 5.9% in Nice, 8.9% in Turin, 32.1% in Valencia, and 48.7% in Wuhan during the lockdown period, while a slight increase (1.8%) in PM_{10} concentration was observed in Rome.

This study has observed substantial differences in $PM_{2.5}$ and PM_{10} reduction across the cities. This can be associated with many factors, including the starting date of lockdown in different cities (Venter et al., 2020), the strictness of the lockdown measures (Singh et al., 2020), traffic volume (Kumar et al., 2020a), uses and mode of domestic energy (EEA, 2019), industrial emission (EEA, 2019), meteorological determinants (Goldberg et al., 2020), etc. Additionally, the reduced level of particulate matter emission can also be linked with the reduction of NO_2, as the indirect conversion from NO_2 to $PM_{2.5}$ was temporarily ceased during the lockdown period. An increased level of $PM_{2.5}$ and PM_{10} concentration was observed in this study in Los Angeles. Chauhan and Singh (2020) observed a similar pattern of air pollution concentration in Los Angeles. Chauhan et al. recorded a 4% reduction in $PM_{2.5}$ in Los Angeles during March 2020, comparing to the baseline period (March 2019), and also noted that such changes are mainly associated with the meteorological factors, i.e., wind speed, wind direction, rainfall, etc. Due to the strong external effects of these confounding factors, air pollution status has been improved in coastal US cities, including the few considered in this study (Goldberg et al., 2020).

The health and economic benefits of the COVID pandemic led to the reduction of air pollution were thoroughly examined across the selected cities. Since we utilized both satellite and in-situ data in the assessment, two relevant valuation approaches, i.e., median externality and public health burden, were implemented for handling the valuation bias and uncertainty. The health impact was presented in terms of ER (excess risk due to exceeding level of air pollution) and health burden (avoided premature mortality due to the reduction of air pollution). The details of RR, ER are given in Table S3, Table S4, Table S5. Combinedly, a total of ~1310 (NO_2), ~401 ($PM_{2.5}$), and ~430 (PM_{10}) cause-specific premature deaths were averted during the study period, which valued ~16 Billion US$. HB was sharply declined from the previous year's baseline. This demonstrates the harmonious association between limited anthropogenic appropriations and resulting economic and health (co)benefits. Kumar et al. (2020a) observation in five Indian cities also found a strong positive association between lockdown restrictions and improved health benefits across the cities. However, Kumar et al. also stated that complete/partial closes of business and industries should not be the optimal way of handling air pollution problems; instead, such an estimate can be treated as a mere supposition to reveal the synergistic association between limited human interferences and associated health/economic (co) benefits.

4.3. Human mobility and its association with air pollution

The connection between human mobility and air pollution levels in selected cities were also examined in this research. Results derived from both Google and Apple mobility report suggested that due to the mandatory lockdown and resulted in limited outdoor human activities, mobility has been reduced significantly across the world. This drastic reduction of human mobility could contribute to the reduced level of air pollution observed in the last few months. For most of the cities analyzed, human mobility has been reduced up to 80% from the baseline mobility. The highest reduction in mobility was found in the European cities. To prevent the spread of the pandemic, the authorities in these cities implemented strong preventive measures, which included partial lockdown in different sectors, including restricted outdoor social activities. This mandatory imposition of lockdown has resulted in a reduced

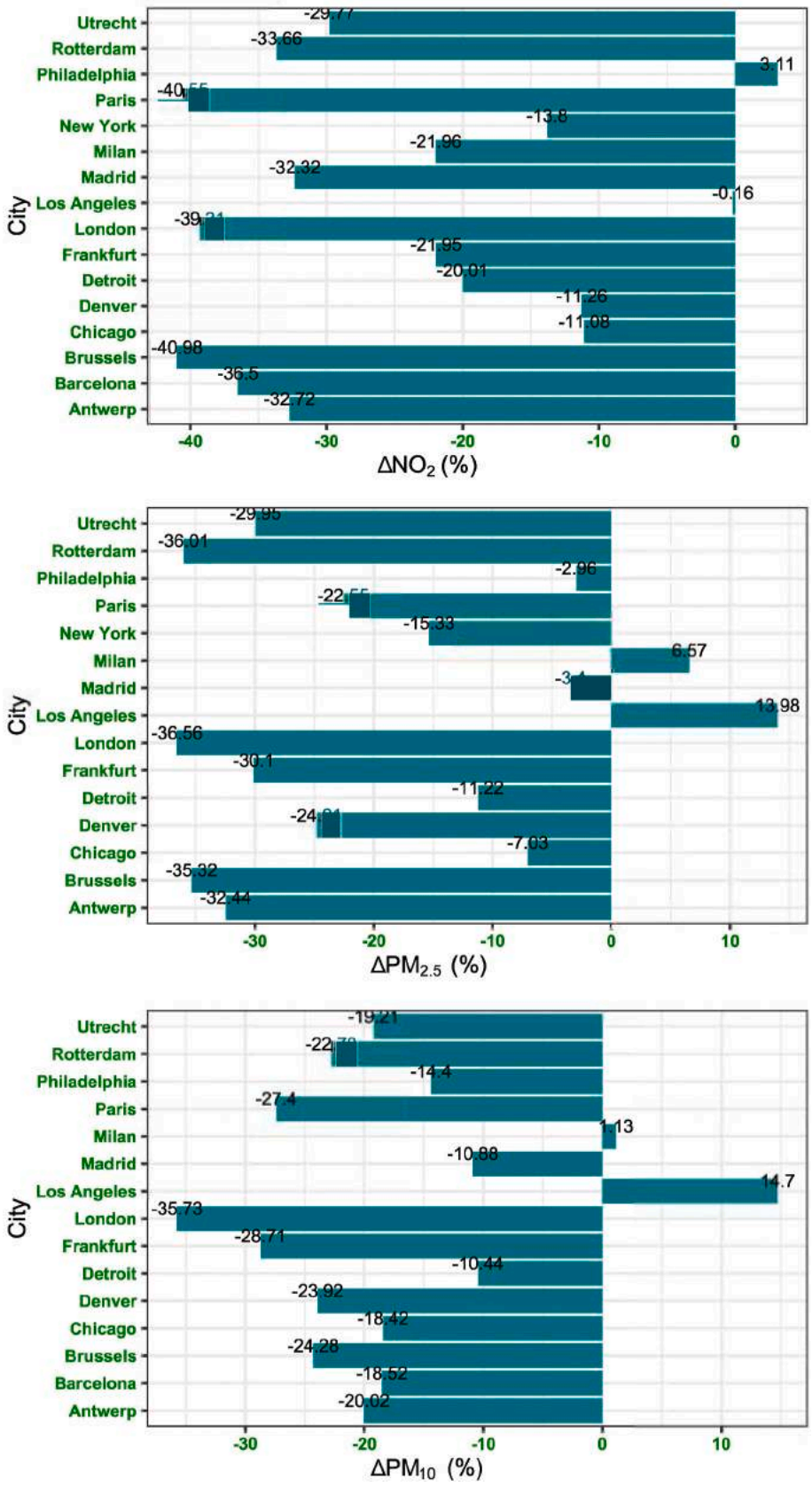

Fig. 7. Changes in NO2, PM2.5, and PM10 concentration (%) during February 1 to May 11 in 2019 and 2020, derived from in-situ data.

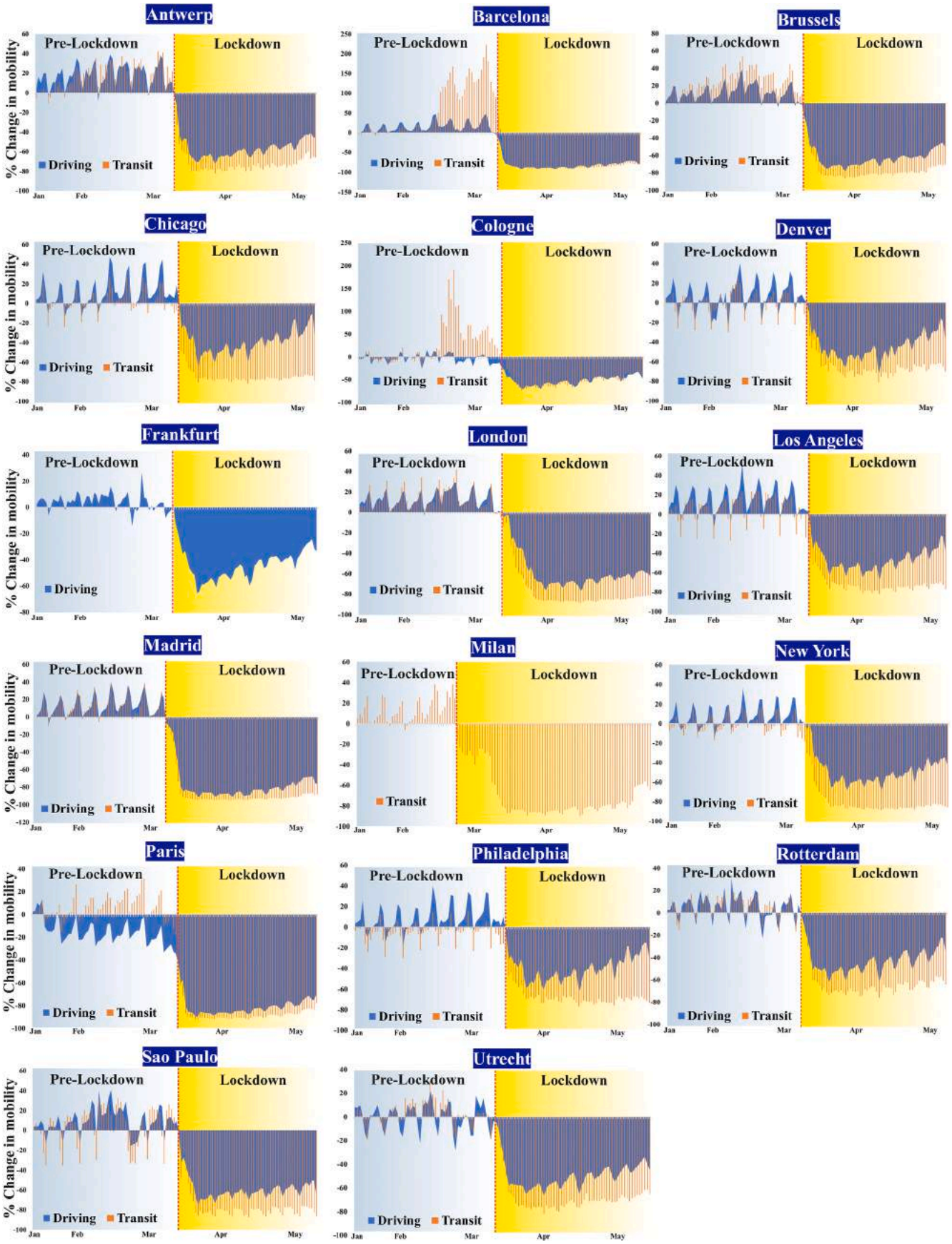

Fig. 8. Changes in mobility due to lock down and resulted in restriction in the selected cities.

Table 3
Per unit ecosystem service equivalent value (US$) of different.

Pollutants	Min	Median	Mean	Max
CO	2	956	956	1931
NO_X	404	1949	5149	17,468
PM_{10}	1747	5149	7907	29,788

Table 4
Economic benefits of reduced anthropogenic emission estimated using median.

City	NO_2	CO	Overall
	Economic Benefit (US$)	Economic Benefit (US$)	Economic Benefit (US$)
Antwerp	2145	2894	5039
Barcelona	1251	2866	4116
Brussels	1720	156	1876
Chicago	8606	4616	13,222
Cologne	5924	−2009	3915
Denver	5115	−6190	−1075
Detroit	6550	16,036	22,585
Frankfurt	4007	1847	5854
London	21,888	17,040	38,928
Los Angeles	5771	14,469	20,240
Madrid	9073	7340	16,413
Milan	4083	5951	10,034
New York	12,976	36,471	49,447
Paris	2362	2608	4971
Philadelphia	5625	13,563	19,188
Rotterdam	3437	−36	3401
Sao Paulo	7415	42,294	49,709
Tehran	31,702	11,923	43,625
Turin	2328	3421	5749
Utrecht	1279	396	1675

level of traffic volume in cities (Fig. 8, Table S2). The mobility analysis thus suggests that by introducing sustainable transport plans and policies, air pollution in the urban regions can be minimized to a certain extent. The periodic and temporary lockdown can also be adopted in highly polluted cities if no other alternatives are feasible to adopt. A similar strategy has already been adopted by New Delhi Government by introducing an "odd/even" transport scheme where private vehicles with odd digit (1, 3, 5, 7, 9) registration numbers will be allowed on roads on odd dates and vehicles with even digit (0, 2, 4, 6, 8) registration numbers can use the vehicles on even dates. Additionally, Mahato et al. study had observed a 40%–50% improvement in air quality in Delhi within the first week of lockdown. He et al. (2020) study on short-term impacts of COVID-19 lockdown on urban air pollution has found that within a week, the AQI in the locked-down cities in China has been reduced by 19.84 points ($PM_{2.5}$ goes down by 14.07 $\mu g/m^3$) compared to the cities where lockdown has not been implemented strictly. The findings suggest an increased clean air ecosystem services in cities under the cessation of human activities.

5. Conclusion

We made an effort to investigate the positive effects of COVID-19 lockdown restrictions on the reduction of NO_2, $PM_{2.5}$, and PM_{10} concentration. Different valuation methods, including median externality and public health burden, were incorporated into the economic valuation to assess the health impact and economic benefits of avoided mortalities. Both satellite and ground-based estimates are exhibiting an affirmative association between controlled human interference and improved air quality. The outcome of this research demonstrates the strong connection between the decline in traffic volume and reduction of NO_2, $PM_{2.5}$, and PM_{10} emission across the cities. This also suggests that the controlled motorized traffic pollution and limiting other unsustainable human activities could be the most effective ways of improving the air quality status of a city. Though the selected pollutants have shown a substantial reduction in all the 20 cities analyzed, there has been an irregularity in the reduction of air pollutants found. Many factors, including meteorological factors, start time of lockdown restrictions, the strictness of lockdown measures, volume of road traffic, other point sources of localized emission, could be linked to this varying concentration and reduction of air pollution observed in the selected cities. The outcome of this study can be a reference to introduce new public policies for promoting adaptive socio-ecological models to understand the synergies and trade-offs between the reduced human interventions and the environmental health of cities systematically. Further research in this direction is needed to explore this synergistic association more explicitly.

Credit author statement

Srikanta Sannigrahi, Conceptualization, Data curation, Formal analysis, Writing – review & editing. Prashant Kumar, Conceptualization, Supervision, Writing – review & editing. Anna Molter, Conceptualization, Writing – review & editing. Qi Zhang, Conceptualization, Writing – review & editing. Bidroha Basu, Conceptualization, Supervision, Writing – review & editing. Arunima Sarkar Basu, Conceptualization, Writing – review & editing. Francesco Pilla, Conceptualization, Supervision, Writing – review & editing.

Table 5
Economic burden (EB) and benefits (Million US$) of reduced anthropogenic emission in NO_2, $PM_{2.5}$, PM_{10}.

City	NO_2			$PM_{2.5}$			PM_{10}		
	EB 2019	EB 2020	Economic Benefit	EB 2019	EB 2020	Economic Benefit	EB 2019	EB 2020	Economic Benefit
Antwerp	616	437	179	413	289	124	442	362	80
Barcelona	1381	933	448	–	–	–	742	615	127
Brussels	296	186	110	167	111	56	155	120	35
Chicago	5486	5002	484	1326	1237	89	2289	1900	389
Denver	1475	1346	128	295	225	70	587	458	130
Detroit	1339	1120	219	331	295	35	411	371	40
Frankfurt	1107	890	217	636	455	181	631	460	171
London	12,815	8395	4420	6034	3955	2078	6319	4200	2119
Los Angeles	8098	8087	10	1682	1906	−224	2643	3001	−358
Madrid	2515	1797	717	810	784	26	964	865	99
Milan	1720	1403	318	1023	1082	−59	984	994	−10
New York	16,907	15,028	1879	3406	2903	502	–	–	–
Paris	2742	1770	972	1329	1052	277	1277	951	326
Philadelphia	2778	2847	−70	694	675	20	954	824	130
Rotterdam	337	236	102	175	116	60	196	154	42
Utrecht	318	232	87	216	155	61	211	173	38

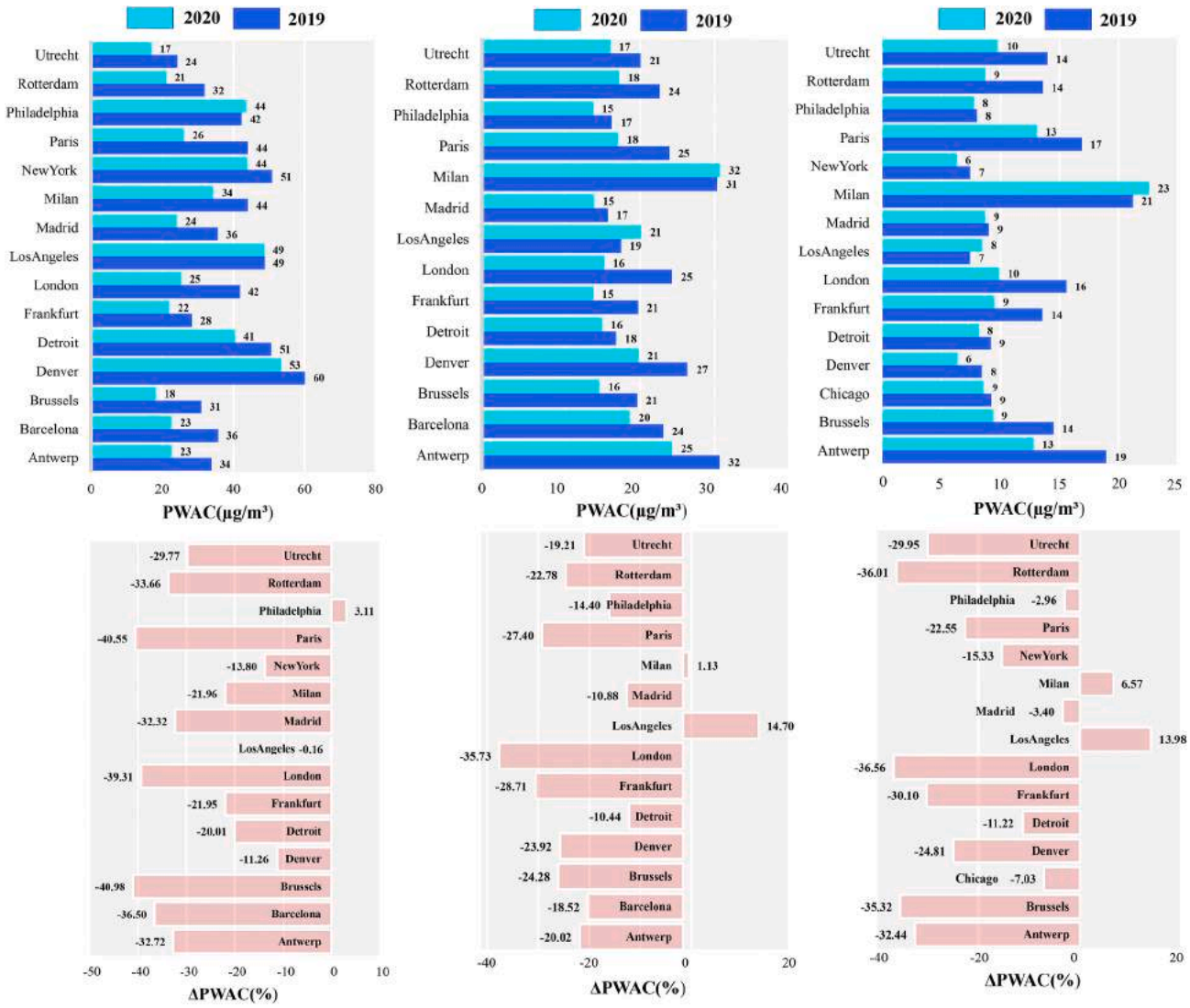

Fig. 9. Population Weighted Average Concentration (PWAC) (μg/m3) for different pollutants in the selected cities.

Declaration of competing interest

The authors declare that they have no known competing financial interests or personal relationships that could have appeared to influence the work reported in this paper.

Acknowledgments

The authors wish to thank the editor and two anonymous reviewers for their constructive comments and suggestions.

Appendix A. Supplementary data

Supplementary data to this article can be found online at https://doi.org/10.1016/j.envres.2021.110927.

References

Our World in Data. https://ourworldindata.org/.

Abhijith, K.V., Kumar, P., Gallagher, J., McNabola, A., Baldauf, R., Pilla, F., Broderick, B., Di Sabatino, S., Pulvirenti, B., 2017. Air pollution abatement performances of green infrastructure in open road and built-up street canyon environments – a review. Atmos. Environ. 162, 71–86. https://doi.org/10.1016/j.atmosenv.2017.05.014.

Alvarez-Mendoza, C.I., Teodoro, A.C., Torres, N., Vivanco, V., 2019. Assessment of remote sensing data to model PM10 Estimation in cities with a low number of air quality stations: a case of Study in Quito, Ecuador. Environments 6 (7), 85.

Apple, 2020. Mobility Trends Reports. https://covid19.apple.com/mobility.

Ash, N., Bennett, K., Reid, W., Irwin, F., Ranganathan, J., Scholes, R., Lee, M., 2010. Assessing ecosystems, ecosystem services, and human well-being. Human Well-Being 1.

Baldasano, J.M., 2020. COVID-19 lockdown effects on air quality by NO_2 in the cities of Barcelona and Madrid (Spain). Sci. Total Environ. 741, 140353.

Bao, R., Zhang, A., 2020. Does lockdown reduce air pollution? Evidence from 44 cities in northern China. Sci. Total Environ. 731, 139052. https://doi.org/10.1016/j.scitotenv.2020.139052.

Baró, F., Chaparro, L., Gómez-Baggethun, E., Langemeyer, J., Nowak, D.J., Terradas, J., 2014. Contribution of ecosystem services to air quality and climate change mitigation policies: the case of urban forests in Barcelona, Spain. Ambio 43, 466–479. https://doi.org/10.1007/s13280-014-0507-x.

Basu, B., Alam, M.S., Ghosh, B., Gill, L., McNabola, A., 2019. In: Augmenting Limited Background Monitoring Data for Improved Performance in Land Use Regression Modelling: Using Support Vector Regression and Mobile Monitoring, vol. 201. Atmospheric Environment, pp. 310–322.

Berman, J.D., Ebisu, K., 2020. Changes in US air pollution during the COVID-19 pandemic. Sci. Total Environ. 739, 139864.

Bherwani, H., Nair, M., Musugu, K., Gautam, S., Gupta, A., Kapley, A., Kumar, R., 2020. Valuation of air pollution externalities: comparative assessment of economic damage and emission reduction under COVID-19 lockdown. Air Qual. Atmos. Heal. 13, 683–694. https://doi.org/10.1007/s11869-020-00845-3.

Borsdorff, T., Aan de Brugh, J., Hu, H., Aben, I., Hasekamp, O., Landgraf, J., 2018. Measuring carbon monoxide with TROPOMI: first results and a comparison with ECMWF-IFS analysis data. Geophys. Res. Lett. 45, 2826–2832. https://doi.org/10.1002/2018GL077045.

Castro, A., Künzli, N., Götschi, T., 2017. Health benefits of a reduction of PM_{10} and NO_2 exposure after implementing a clean air plan in the Agglomeration Lausanne-Morges. Int. J. Hyg Environ. Health 220, 829–839. https://doi.org/10.1016/j.ijheh.2017.03.012.

Chan, C.K., Yao, X., 2008. Air pollution in mega cities in China. Atmos. Environ. 42, 1–42. https://doi.org/10.1016/j.atmosenv.2007.09.003.

Charles, M., Ziv, G., Bohrer, G., Bakshi, B.R., 2020. Connecting air quality regulating ecosystem services with beneficiaries through quantitative serviceshed analysis. Ecosyst. Serv. 41, 101057. https://doi.org/10.1016/j.ecoser.2019.101057.

Chauhan, A., Singh, R.P., 2020. Decline in $PM_{2.5}$ concentrations over major cities around the world associated with COVID-19. In: Environmental Research, vol. 187. Elsevier Inc., p. 109634. https://doi.org/10.1016/j.envres.2020.109634

Chen, K., Wang, M., Huang, C., Kinney, P.L., Anastas, P.T., 2020. Air pollution reduction and mortality benefit during the COVID-19 outbreak in China. Lancet Planet. Heal. 2019 https://doi.org/10.1016/S2542-5196(20)30107-8, 2019–2021.

Chinazzi, M., Davis, J.T., Ajelli, M., Gioannini, C., Litvinova, M., Merler, S., Pastore y Piontti, A., Mu, K., Rossi, L., Sun, K., Viboud, C., Xiong, X., Yu, H., Halloran, M.E., Longini, I.M., Vespignani, A., 2020. The effect of travel restrictions on the spread of the 2019 novel coronavirus (COVID-19) outbreak. Science 368, 395. https://doi.org/10.1126/science.aba9757.

COMEAP, 2010. The mortality effects of long term exposure to particulate AirPollution in the UK. Report Produced by the Health Protection Agency for theCommittee on the Medical Effects of Air Pollutants 98.

Connerton, P., Vicente de Assunção, J., Maura de Miranda, R., Dorothée Slovic, A., José Pérez-Martínez, P., Ribeiro, H., 2020. Air quality during COVID-19 in four megacities: lessons and challenges for public health. Int. J. Environ. Res. Publ. Health 17 (14), 5067.

Crouse, D.L., Peters, P.A., Hystad, P., Brook, J.R., van Donkelaar, A., Martin, R.V., Villeneuve, P.J., Jerrett, M., Goldberg, M.S., Pope III, C.A., Brauer, M., 2015. Ambient PM2. 5, O3, and NO2 exposures and associations with mortality over 16 years of follow-up in the Canadian census health and environment cohort (CanCHEC). Environ. Health Perspect. 123, 1180–1186. https://doi.org/10.1289/ehp.1409276.

De Brouwer, E., Raimondi, D., Moreau, Y., 2020. Modeling the COVID-19 outbreaks and the effectiveness of the containment measures adopted across countries. medRxiv. https://doi.org/10.1101/2020.04.02.20046375.

Drake, T.M., Docherty, A.B., Weiser, T.G., Yule, S., Sheikh, A., Harrison, E.M., 2020. The effects of physical distancing on population mobility during the COVID-19 pandemic in the UK. The Lancet Digital Health 2 (8), e385–e387.

Dutheil, F., Baker, J.S., Navel, V., 2020a. COVID-19 as a factor influencing air pollution? Environ. Pollut. 263 https://doi.org/10.1016/j.envpol.2020.114466.

Dutheil, F., Baker, J.S., Navel, V., 2020b. COVID-19 as a factor influencing air pollution? Environ. Pollut. 263, 114466. https://doi.org/10.1016/j.envpol.2020.114466.

Etchie, T.O., Etchie, A.T., Adewuyi, G.O., Pillarisetti, A., Sivanesan, S., Krishnamurthi, K., Arora, N.K., 2018. The gains in life expectancy by ambient $PM_{2.5}$ pollution reductions in localities in Nigeria. Environ. Pollut. 236, 146–157. https://doi.org/10.1016/j.envpol.2018.01.034.

European Environmental Agency, 2019. Contribution of the Transport Sector to Total Emissions of the Main Air Pollutants. https://www.eea.europa.eu/data-and-maps/daviz/contribution-of-the-transport-sector-6#tab-chart_4.

European Space Agency, 2020. https://www.esa.int/Applications/Observing_the_Earth/Co-pernicus/Sentinel-5P.

Feng, L., Liao, W., 2016. Legislation, plans, and policies for prevention and control of air pollution in China: achievements, challenges, and improvements. J. Clean. Prod. 112, 1549–1558. https://doi.org/10.1016/j.jclepro.2015.08.013.

Fernández-Pacheco, V.M., López-Sánchez, C.A., Álvarez-Álvarez, E., López, M.J., García-Expósito, L., Yudego, E.A., Carús-Candás, J.L., 2018. Estimation of PM10 distribution using Landsat5 and Landsat8 remote sensing. In: Multidisciplinary Digital, vol. 2. Publishing Institute Proceedings, p. 1430.

Fierens, F., 2011. Air pollution in Belgium: will we be able to comply with the European standards? Verh. - K. Acad. Geneeskd. Belg. 73 (5–6), 353–359.

Gautam, S., 2020. The influence of COVID-19 on air quality in India: a boon or inutile. Bull. Environ. Contam. Toxicol. 104, 724–726. https://doi.org/10.1007/s00128-020-02877-y.

Goldberg, D.L., Anenberg, S.C., Griffin, D., McLinden, C.A., Lu, Z., Streets, D.G., 2020. Disentangling the impact of the COVID-19 lockdowns on urban NO_2 from natural variability. Geophys. Res. Lett. 47 (17), e2020GL089269.

Google, 2020. Community Mobility Reports. https://www.google.com/covid19/mobility/.

Griffin, D., Zhao, X., McLinden, C.A., Boersma, F., Bourassa, A., Dammers, E., Degenstein, D., Eskes, H., Fehr, L., Fioletov, V., Hayden, K., Kharol, S.K., Li, S.-M., Makar, P., Martin, R.V., Mihele, C., Mittermeier, R.L., Krotkov, N., Sneep, M., Lamsal, L.N., Linden, M. ter, Geffen, J. van, Veefkind, P., Wolde, M., 2019. High-resolution mapping of nitrogen dioxide with TROPOMI: first results and validation over the Canadian oil sands. Geophys. Res. Lett. 46, 1049–1060. https://doi.org/10.1029/2018GL081095.

Guanter, L., Aben, I., Tol, P., Krijger, J.M., Hollstein, A., Köhler, P., Damm, A., Joiner, J., Frankenberg, C., Landgraf, J., 2015. Potential of the TROPOspheric Monitoring Instrument (TROPOMI) onboard the Sentinel-5 Precursor for the monitoring of terrestrial chlorophyll fluorescence. Atmos. Meas. Tech. 8, 1337–1352. https://doi.org/10.5194/amt-8-1337-2015.

Guerriero, C., Chatzidiakou, L., Cairns, J., Mumovic, D., 2016. The economic benefits of reducing the levels of nitrogen dioxide (NO_2) near primary schools: the case of London. J. Environ. Manag. 181, 615–622. https://doi.org/10.1016/j.jenvman.2016.06.039.

Guevara, M., Jorba, O., Soret, A., Petetin, H., Bowdalo, D., Serradell, K., Tena, C., Denier van der Gon, H., Kuenen, J., Peuch, V.H., Pérez García-Pando, C., 2020. Time-resolved emission reductions for atmospheric chemistry modelling in Europe during the COVID-19 lockdowns. Atmos. Chem. Phys. Discuss. 1–37.

Guttikunda, S.K., Goel, R., Pant, P., 2014. Nature of air pollution, emission sources, and management in the Indian cities. Atmos. Environ. 95, 501–510. https://doi.org/10.1016/j.atmosenv.2014.07.006.

He, G., Pan, Y., Tanaka, T., 2020. The short-term impacts of COVID-19 lockdown on urban air pollution in China. Nat. Sustain. https://doi.org/10.1038/s41893-020-0581-y.

He, L., Zhang, S., Hu, J., Li, Z., Zheng, X., Cao, Y., Xu, G., Yan, M., Wu, Y., 2020. On-road emission measurements of reactive nitrogen compounds from heavy-duty diesel trucks in China. Environ. Pollut. 262, 114280. https://doi.org/10.1016/j.envpol.2020.114280.

Hu, J., Ying, Q., Wang, Y., Zhang, H., 2015. Characterising multi-pollutant air pollution in China: comparison of three air quality indices. Environ. Int. 84, 17–25. https://doi.org/10.1016/j.envint.2015.06.014.

Ialongo, I., Virta, H., Eskes, H., Hovila, J., Douros, J., 2020. Comparison of TROPOMI/Sentinel-5 Precursor NO 2 observations with ground-based measurements in Helsinki. Atmospheric Measurement Techniques 13 (1), 205–218.

Institute for Health Metrics and Evaluation, 2018. Findings from the Global Burden of Disease Study 2017. IHME, Seattle, WA.

Ivy, D., Mulholland, J.A., Russell, A.G., 2008. Development of ambient air quality population-weighted metrics for use in time-series health studies. J. Air Waste Manag. Assoc. 58 (5), 711–720.

Jeanjean, A.P.R., Gallagher, J., Monks, P.S., Leigh, R.J., 2017. Ranking current and prospective NO_2 pollution mitigation strategies: an environmental and economic modelling investigation in Oxford Street, London. Environ. Pollut. 225, 587–597. https://doi.org/10.1016/j.envpol.2017.03.027.

Kanniah, K.D., Kamarul Zaman, N.A.F., Kaskaoutis, D.G., Latif, M.T., 2020. COVID-19's impact on the atmospheric environment in the Southeast Asia region. Sci. Total Environ. 736, 139658. https://doi.org/10.1016/j.scitotenv.2020.139658.

Kaplan, G., Yigit Avdan, Z., 2020. Space-borne air pollution observation from sentinel-5P tropomi: relationship between pollutants, geographical and demographic data. Int. J. Eng. Geosci. 130–137. https://doi.org/10.26833/ijeg.644089.

Kerimray, A., Baimatova, N., Ibragimova, O.P., Bukenov, B., Kenessov, B., Plotitsyn, P., Karaca, F., 2020. Assessing air quality changes in large cities during COVID-19 lockdowns: the impacts of traffic-free urban conditions in Almaty, Kazakhstan. Sci. Total Environ. 730, 139179.

Kim Oanh, N.T., Upadhyay, N., Zhuang, Y.-H., Hao, Z.-P., Murthy, D.V.S., Lestari, P., Villarin, J.T., Chengchua, K., Co, H.X., Dung, N.T., Lindgren, E.S., 2006. Particulate air pollution in six Asian cities: spatial and temporal distributions, and associated sources. Atmos. Environ. 40, 3367–3380. https://doi.org/10.1016/j.atmosenv.2006.01.050.

Kloog, I., Nordio, F., Coull, B.A., Schwartz, J., 2012. Incorporating local land use regression and satellite aerosol optical depth in a hybrid model of spatiotemporal PM2. 5 exposures in the Mid-Atlantic states. Environ. Sci. Technol. 46 (21), 11913–11921.

Kumar, P., Lidia, M., 2019. Could fighting airborne transmission be the next line of defence against COVID-19 spread? City and Environment Interactions 4, 100033.

Kumar, P., Khare, M., Harrison, R.M., Bloss, W.J., Lewis, A., Coe, H., Morawska, L., 2015. New directions: air pollution challenges for developing megacities like Delhi. Atmos. Environ. 122, 657–661.

Kumar, P., Andrade, M.F., Ynoue, R.Y., Fornaro, A., de Freitas, E.D., Martins Martins, J.L. D., Albuquerque, T., Zhang, Y., Morawska, L., 2016. New Directions: from biofuels to wood stoves: the modern and ancient air quality challenges in the megacity of São Paulo. Atmos. Environ. 140, 364–369.

Kumar, P., Druckman, A., Gallagher, J., Gatersleben, B., Allison, S., Eisenman, T.S., Hoang, U., Hama, S., Tiwari, A., Sharma, A., Abhijith, K.V., Adlakha, D., McNabola, A., Astell-Burt, T., Feng, X., Skeldon, A.C., de Lusignan, S., Morawska, L., 2019. The nexus between air pollution, green infrastructure and human health. Environ. Int. 133, 105181.

Kumar, P., Hama, S., Omidvarborna, H., Sharma, A., Sahani, J., Abhijith, K.V., Debele, S., Zavala-Reyes, J., Barwise, Y., Tiwari, A., 2020. Temporary reduction in fine particulate matter due to 'anthropogenic emissions switch-off' during COVID-19 lockdown in Indian cities. Sustain. Cities Soc. 62, 102382. https://doi.org/10.1016/j.scs.2020.102382.

Kumar, P., Hama, S., Nogueira, T., Abbass, R.A., Brand, V.S., Andrade, M.F., Asfaw, A., Aziz, K.H., Cao, S.J., El-Gendy, A., Islam, S., Jeba, F., Khare, M., Mamuya, S.H., Martinez, J., Meng, M.R., Morawska, L., Muula, A.S., Sm, S.N., Ngowi, A.V., Omer, K., Olaya, Y., Osano, P., Salam, A., 2021. In-car particulate matter exposure across ten global cities. Sci. Total Environ. 750, 141395.

Liu, M., Lin, J., Kong, H., Boersma, K.F., Eskes, H., Kanaya, Y., He, Q., Tian, X., Qin, K., Xie, P., Spurr, R., 2020. A new TROPOMI product for tropospheric NO 2 columns over East Asia with explicit aerosol corrections. Atmospheric Measurement Techniques 13 (8), 4247–4259.

Lorente, A., Boersma, K.F., Eskes, H.J., Veefkind, J.P., van Geffen, J.H.G.M., de Zeeuw, M.B., Denier van der Gon, H.A.C., Beirle, S., Krol, M.C., 2019. Quantification of nitrogen oxides emissions from build-up of pollution over Paris with TROPOMI. Sci. Rep. 9, 20033. https://doi.org/10.1038/s41598-019-56428-5.

Mahato, S., Pal, S., Ghosh, K.G., 2020. Effect of lockdown amid COVID-19 pandemic on air quality of the megacity Delhi, India. Sci. Total Environ. 730, 139086. https://doi.org/10.1016/j.scitotenv.2020.139086.

Matthews, H.S., Lave, L.B., 2000. Applications of environmental valuation for determining externality costs. Environ. Sci. Technol. 34, 1390–1395. https://doi.org/10.1021/es9907313.

Mayer, H., 1999. Air pollution in cities. Atmos. Environ. 33, 4029–4037. https://doi.org/10.1016/S1352-2310(99)00144-2.
Mehta, M., Singh, R., Singh, A., Singh, N., 2016. Recent global aerosol optical depth variations and trends—a comparative study using MODIS and MISR level 3 datasets. Remote Sens. Environ. 181, 137–150.
Meng, X., Fu, Q., Ma, Z., Chen, L., Zou, B., Zhang, Y., Xue, W., Wang, J., Wang, D., Kan, H., Liu, Y., 2016. Estimating ground-level PM10 in a Chinese city by combining satellite data, meteorological information and a land use regression model. Environ. Pollut. 208, 177–184.
Millennium Ecosystem Assessment, 2005. Ecosystems and Human Well-Being: Synthesis. Island Press, Washington, DC).
Monica, C., Ennio, C., Massimo, S., Claudia, G., Giovanna, B., Annunziata, F., Luigi, B., Angela, V.M., Patrizia, D.M., Achille, C., Sandra, M., Barbara, P., Sante, M., Lorenzo, S., Francesco, F., null, null, 2011. Short-term effects of nitrogen dioxide on mortality and susceptibility factors in 10 Italian cities: the EpiAir study. Environ. Health Perspect. 119, 1233–1238. https://doi.org/10.1289/ehp.1002904.
Muhammad, S., Long, X., Salman, M., 2020. COVID-19 pandemic and environmental pollution: a blessing in disguise? Sci. Total Environ. 728, 138820. https://doi.org/10.1016/j.scitotenv.2020.138820.
Ogen, Y., 2020. Assessing nitrogen dioxide (NO_2) levels as a contributing factor to coronavirus (COVID-19) fatality. Sci. Total Environ. 726, 138605. https://doi.org/10.1016/j.scitotenv.2020.138605.
Ortiz, C., Linares, C., Carmona, R., Díaz, J., 2017. Evaluation of short-term mortality attributable to particulate matter pollution in Spain. Environ. Pollut. 224, 541–551. https://doi.org/10.1016/j.envpol.2017.02.037.
Otmani, A., Benchrif, A., Tahri, M., Bounakhla, M., Chakir, E.M., El Bouch, M., Krombi, M., 2020. Impact of covid-19 lockdown on PM_{10}, SO_2 and NO_2 concentrations in salé city (Morocco). Sci. Total Environ. 735, 139541. https://doi.org/10.1016/j.scitotenv.2020.139541.
Park, J., Jo, W., Cho, M., Lee, J., Lee, H., Seo, S., Lee, C., Yang, W., 2020. Spatial and temporal exposure assessment to PM2. 5 in a community using sensor-based air monitoring instruments and dynamic population distributions. Atmosphere 11 (12), 1284.
Pilla, F., Broderick, B., 2015. A GIS model for personal exposure to PM_{10} for Dublin commuters. Sustain. Cities Soc. 15, 1–10. https://doi.org/10.1016/j.scs.2014.10.005.
Rai, A.C., Kumar, P., Pilla, F., Skouloudis, A.N., Di Sabatino, S., Ratti, C., Yasar, A., Rickerby, D., 2017. End-user perspective of low-cost sensors for outdoor air pollution monitoring. Sci. Total Environ. 607 (608), 691–705. https://doi.org/10.1016/j.scitotenv.2017.06.266.
Rodríguez-Urrego, D., Rodríguez-Urrego, L., 2020. Air quality during the COVID-19: $PM_{2.5}$ analysis in the 50 most polluted capital cities in the world. In: Environmental Pollution, vol. 266. Elsevier Ltd, p. 115042. https://doi.org/10.1016/j.envpol.2020.115042.
Rohde, R.A., Muller, R.A., 2015. Air pollution in China: mapping of concentrations and sources. PloS One 10, e0135749.
Sahu, S.K., Kota, S.H., 2017. Significance of $PM_{2.5}$ air quality at the Indian capital. Aerosol Air Qual. Res. 17, 588–597. https://doi.org/10.4209/aaqr.2016.06.0262.
Sannigrahi, S., Pilla, F., Basu, B., Basu, A.S., Molter, A., 2020. Examining the Association between Socio-Demographic Composition and COVID-19 Fatalities in the European Region Using Spatial Regression Approach. Sustainable Cities and Society, p. 102418.
Sasidharan, M., Singh, A., Torbaghan, M.E., Parlikad, A.K., 2020. A vulnerability-based approach to human-mobility reduction for countering COVID-19 transmission in London while considering local air quality. Sci. Total Environ. 741, 140515. https://doi.org/10.1016/j.scitotenv.2020.140515.
Schirpke, U., et al., 2014. Mapping Beneficiaries of Ecosystem Services Flows from Natura 2000 Sites, vol. 9. Ecosystem Services, pp. 170–179. https://doi.org/10.1016/j.ecoser.2014.06.003.
SEDAC, NASA, 2020. Gridded population of the world, version 4 (GPWv4): population density. In: NASA Socioeconomic Data and Applications Center (SEDAC).
Sharma, S., Zhang, M., Anshika Gao, J., Zhang, H., Kota, S.H., 2020. Effect of restricted emissions during COVID-19 on air quality in India. Sci. Total Environ. 728, 138878. https://doi.org/10.1016/j.scitotenv.2020.138878.
Shehzad, K., Sarfraz, M., Shah, S.G.M., 2020. The impact of COVID-19 as a necessary evil on air pollution in India during the lockdown. Environ. Pollut. 266, 115080. https://doi.org/10.1016/j.envpol.2020.115080.
Shikwambana, L., Mhangara, P., Mbatha, N., 2020. Trend analysis and first time observations of sulphur dioxide and nitrogen dioxide in South Africa using TROPOMI/Sentinel-5 P data. Int. J. Appl. Earth Obs. Geoinf. 91, 102130. https://doi.org/10.1016/j.jag.2020.102130.
Sicard, P., De Marco, A., Agathokleous, E., Feng, Z., Xu, X., Paoletti, E., Rodriguez, J.J.D., Calatayud, V., 2020. Amplified ozone pollution in cities during the COVID-19 lockdown. Sci. Total Environ. 735 https://doi.org/10.1016/j.scitotenv.2020.139542.
Singh, V., Singh, S., Biswal, A., Kesarkar, A.P., Mor, S., Ravindra, K., 2020. Diurnal and temporal changes in air pollution during COVID-19 strict lockdown over different regions of India. Environ. Pollut. 266, 115368.
Theys, N., Hedelt, P., De Smedt, I., Lerot, C., Yu, H., Vlietinck, J., Pedergnana, M., Arellano, S., Galle, B., Fernandez, D., Carlito, C.J.M., Barrington, C., Taisne, B., Delgado-Granados, H., Loyola, D., Van Roozendael, M., 2019. Global monitoring of volcanic SO_2 degassing with unprecedented resolution from TROPOMI onboard Sentinel-5 Precursor. Sci. Rep. 9, 2643. https://doi.org/10.1038/s41598-019-39279-y.
Troko, J., Myles, P., Gibson, J., Hashim, A., Enstone, J., Kingdon, S., Packham, C., Amin, S., Hayward, A., Van-Tam, J.N., 2011. Is public transport a risk factor for acute respiratory infection? BMC Infect. Dis. 11, 16. https://doi.org/10.1186/1471-2334-11-16.
TROPOMI Explorer. An application to visualize air pollutant time series data. https://showcase.earthengine.app/view/tropomi-explorer.
United States Environmental Protection Agency. Outdoor Air Quality Data. https://www.epa.gov/outdoor-air-quality-data/download-daily-data.
U.S Bureau of Labor Statistics, 2020. https://www.bls.gov/data/inflation_calculator.htm.
Valade, S., Ley, A., Massimetti, F., D'Hondt, O., Laiolo, M., Coppola, D., Loibl, D., Hellwich, O., Walter, T.R., 2019. Towards global volcano monitoring using multisensor sentinel missions and artificial intelligence: the MOUNTS monitoring system. Rem. Sens. 11, 1–31. https://doi.org/10.3390/rs11131528.
Veefkind, J.P., Aben, I., McMullan, K., Förster, H., de Vries, J., Otter, G., Claas, J., Eskes, H.J., de Haan, J.F., Kleipool, Q., van Weele, M., Hasekamp, O., Hoogeveen, R., Landgraf, J., Snel, R., Tol, P., Ingmann, P., Voors, R., Kruizinga, B., Vink, R., Visser, H., Levelt, P.F., 2012. TROPOMI on the ESA Sentinel-5 Precursor: a GMES mission for global observations of the atmospheric composition for climate, air quality and ozone layer applications. Remote Sens. Environ. 120, 70–83. https://doi.org/10.1016/j.rse.2011.09.027.
Venter, Z.S., Aunan, K., Chowdhury, S., Lelieveld, J., 2020. COVID-19 lockdowns cause global air pollution declines with implications for public health risk. medRxiv. https://doi.org/10.1101/2020.04.10.20060673.
Viscusi, W.K., Masterman, C.J., 2017. Income elasticities and global values of a statistical life. J. Benefit-Cost Anal. 8, 226–250. https://doi.org/10.1017/bca.2017.12.
Wang, S., Hao, J., 2012. Air quality management in China: issues, challenges, and options. J. Environ. Sci. 24, 2–13. https://doi.org/10.1016/S1001-0742(11)60724-9.
Wang, H., Yamamoto, N., 2020. Using a partial differential equation with Google Mobility data to predict COVID-19 in Arizona. Math. Biosci. Eng. 17 (5).
Wang, P., Chen, K., Zhu, S., Wang, P., Zhang, H., 2020. Severe air pollution events not avoided by reduced anthropogenic activities during COVID-19 outbreak. Resour. Conserv. Recycl. 158, 104814.
Wellenius, G.A., Vispute, S., Espinosa, V., Fabrikant, A., Tsai, T.C., Hennessy, J., Williams, B., Gadepalli, K., Boulange, A., Pearce, A., Kamath, C., 2020. Impacts of State-Level Policies on Social Distancing in the United States Using Aggregated Mobility Data during the COVID-19 Pandemic.
WHO, 2020. Director-General's Opening Remarks at the Media Briefing on COVID. https://www.who.int/director-general/speeches/detail/who-director-general-s-opening-remarks-at-the-media-briefing-on-covid-19—11-may-2020.
Yilmazkuday, H., 2020. Stay-at-home works to fight against COVID-19: international evidence from Google mobility data. J. Hum. Behav. Soc. Environ. 1–11.
Zeng, P., Lyu, X.P., Guo, H., Cheng, H.R., Jiang, F., Pan, W.Z., Wang, Z.W., Liang, S.W., Hu, Y.Q., 2018. Causes of ozone pollution in summer in Wuhan, Central China. Environ. Pollut. 241, 852–861.
Zhang, J., Reid, J.S., 2010. A decadal regional and global trend analysis of the aerosol optical depth using a data-assimilation grade over-water MODIS and Level 2 MISR aerosol products. Atmos. Chem. Phys. 10 (22), 10949–10963.
Zhang, H., Wang, Shuxiao, Hao, J., Wang, X., Wang, Shulan, Chai, F., Li, M., 2016. Air pollution and control action in Beijing. J. Clean. Prod. 112, 1519–1527. https://doi.org/10.1016/j.jclepro.2015.04.092.
Zhang, Q., Song, C., Chen, X., 2018. Effects of China's payment for ecosystem services programs on cropland abandonment: a case study in Tiantangzhai Township, Anhui, China. Land Use Pol. 73, 239–248.
Zhang, B., Zhang, M., Kang, J., Hong, D., Xu, J., Zhu, X., 2019. Estimation of pmx concentrations from landsat 8 oli images based on a multilayer perceptron neural network. Rem. Sens. 11 (6), 646.
Zhang, Q., Wang, Y., Tao, S., Bilsborrow, R.E., Qiu, T., Liu, C., Sannigrahi, S., Li, Q., Song, C., 2020. Divergent socioeconomic-ecological outcomes of China's conversion of cropland to forest program in the subtropical mountainous area and the semi-arid Loess Plateau. Ecosystem Services 45, 101167.
Zheng, Z., Yang, Z., Wu, Z., Marinello, F., 2019. Spatial variation of NO_2 and its impact factors in China: an application of sentinel-5P products. Rem. Sens. 11, 1–24. https://doi.org/10.3390/rs11161939.
Zhu, Y., Xie, J., Huang, F., Cao, L., 2020. Association between short-term exposure to air pollution and COVID-19 infection: evidence from China. Sci. Total Environ. 727, 138704. https://doi.org/10.1016/j.scitotenv.2020.138704.
Zoran, M.A., Savastru, R.S., Savastru, D.M., Tautan, M.N., 2020. Assessing the relationship between surface levels of $PM_{2.5}$ and PM_{10} particulate matter impact on COVID-19 in Milan. Italy. Sci. Total Environ. 738, 139825.